Mechanical characterization of modern concrete masonry elements

by

Justin Di Costa

December 11th, 2024

Department of Civil Engineering and Applied Mechanics

McGill University

Montreal, QC

A thesis submitted to McGill University in partial fulfillment of the requirements of the degree of Master of Science

Abstract

As the demands for sustainable construction practices grows, the durability of modern concrete masonry components such as loadbearing concrete blocks and metal wall ties in cavity wall systems becomes increasingly critical. This paper investigates the mechanical properties of hollow concrete masonry specimens and their interaction with cavity wall ties given that certain aspects of the compressive behaviour of concrete block masonry and ties are under-researched. There is especially limited data on the compressive strength relationship between the bond pattern and size effects of masonry block assemblies. Also, there is a need to further explore the loading on varying lengths of modern adjustable wall ties due to the trend for wider wall cavities that serve to promote better insulation and mitigate the predicted variations in temperatures due to climate change. The study will explore uniaxial compression testing of concrete masonry consisting of variations in height bonding patterns (stack and running bond), as well as the evaluation of adjustable wall ties at different lengths and varying positions under tension and compression loads. These tests will conform to, among others, the guidelines highlighted in CSA S304-14 (Design of masonry structures) and CSA A370-14 (Connectors for masonry). By examining both the compressive strength of masonry block specimens and the load-resistance capabilities of wall ties, this research aims to enhance the understanding of the individual component properties, and the resulting combined effects found in masonry structures. This study is part of a larger research project at McGill University on implications from climate change and resilience of materials in structural design. These findings could potentially influence and support updates to CSA standards and provide manufacturers with valuable knowledge to enhance product performance and durability. Ultimately, this study aims to fortify concrete masonry elements against environmental challenges, advancing sustainable construction practices and contributing to the evolution of masonry construction materials.

Résumé

Alors que la demande pour des pratiques de construction durables augmente, la durabilité des composants modernes en maçonnerie de béton devient de plus en plus cruciale, comme les blocs de béton porteurs et les ancrages métalliques dans les systèmes de murs creux. Cette thèse examine les propriétés mécaniques des spécimens de bloc en béton (creux) et leur interaction avec les ancrages de mur creux, car certains aspects du comportement en compression de la maçonnerie en blocs de béton et des ancrages sont peu étudiés. Il existe notamment des données limitées sur la relation entre la résistance à la compression, le mode de construction et les effets de taille sur les assemblages de blocs de maçonnerie, ainsi sur les charges appliquées à des ancrages ajustable modernes de longueurs variables, en raison du besoin de cavités murales plus larges pour favoriser une meilleure isolation et atténuer les variations de température prévues en raison du changement climatique. L'étude explorera les essais de compression uni-axiale de maçonnerie en béton avec des variations de hauteurs et de mode de liaison (liaison empilée et liaison en croix), ainsi l'évaluation des ancrages ajustable à différentes longueurs et positions de charge sous des charges de tension et compression. Ces essais seront, entre autres, conformes aux directives de la norme CSA S304 (Conception des structures en maçonnerie) et de la norme CSA A370 (Connecteurs pour maçonnerie). En examinant à la fois la résistance à la compression des spécimens de blocs de maçonnerie et la capacité de résistance aux charges des ancrages, cette recherche vise à améliorer la compréhension des effets matériels et combinés présents dans les structures en maçonnerie. Cette étude fait partie d'un projet de recherche plus large à l'Université McGill sur les implications du changement climatique et la résilience des matériaux dans la conception des structures. Ces résultats pourraient potentiellement influencer et appuyer les mises à jour des normes CSA et fournir aux fabricants des connaissances précieuses pour améliorer la performance et la durabilité des produits. En fin de compte, cette étude vise à renforcer les éléments de maçonnerie en béton contre les défis environnementaux, à promouvoir des pratiques de construction durables et à contribuer à l'évolution des matériaux de construction en maçonnerie.

Acknowledgement

My research work over the past two years wouldn't have been possible without my supervisor Professor Daniele Malomo. He was an integral part of my academic, research and career growth as a professional in the field of engineering. The competence he demonstrated in masonry related products and his overall engineering expertise was crucial in transferring his knowledge to my experimental work. He was always available for meetings and provided insight into potential challenges I faced throughout my research, along with creating a great working environment consisting of a large research group with multiple research projects. Professor Malomo is a dedicated teacher and an important mentor that has shaped my work ethic, advanced my knowledge and has contributed to the professionalism that will help guide and build my career.

I would also like to thank Adrien Sparling from the Canada Masonry Design Centre (CMDC), our industry partner for this research, for his valuable insights, prompt responses to my questions, and participation in meetings which positively contributed to my understanding of key concepts. Furthermore, I am grateful to the laboratory technicians: John Bartczak, Mike Stephens, and William Cook, whose assistance in test setup preparations was instrumental in meeting the research needs, safety guidelines and project timelines.

Finally, I would like to express my gratitude to McGill University for awarding me the MEUSMA scholarship. I am also thankful to the CSA Group for their financial support through the CSA Group Graduate Scholarship, as well as for providing access to their standards, which were essential to the completion of my research.

Table of contents

List of figures

List of tables

1 Introduction

1.1 Overview of masonry cavity walls consisting of concrete blocks and wall ties

Early use of masonry cavity walls was different than the ones in current structures around the globe. Masonry cavity walls in the early 19th century consisted of two brick walls, one wall acting as a veneer and other wall as loadbearing envelope which was separated by a cavity and connected with brick headers laid on edge as seen in Figure 1.1. This type of bond is commonly referred to as a ‘rat trap bond’. These walls are the exterior structural loadbearing walls which shelter the interior of small buildings. It was later realized that having the brick header tying the two walls together provided a disadvantage to the integrity of the structure since the brick allowed for moisture to travel into the building envelope causing moisture induced damage and structural performance issues in freeze thaw cycles. In the 1840’s, thin metal cavity wall ties were first used as a replacement for the header bricks and these ties were typically made of cast iron or wrought iron with most homes in England being made with metal tie connected building envelopes. The ties were placed in between brick mortar joints; however, these types of ties were susceptible to corrosion and inevitable failure of walls caused by inadequate load transfer as seen in Figure 1.2. Builders developed galvanized ties of various shapes and sizes. (Giaretton, Dizhur et al. 2016).

Figure 1.1. Rat trap bond masonry construction (THE CONSTRUCTOR 2020)

Figure 1.2. Corrosion of thin metal ties in small width cavity walls (Giaretton, Dizhur et al. 2016)

These ties were present in North America in the late 19th century with the cavity walls being constructed with a brick veneer and concrete masonry block units (CMU) as the loadbearing interior walls. The air in the cavity was used as the main insulator since air has a very low thermal conductivity, which means it does not easily transfer heat and makes it an ideal effective barrier to heat flow between the exterior and interior of structures. The past cavities typically measured around 50 mm in width. (DiDomizio, Quintana-Morales et al. 2024). The loadbearing backup part of the cavity wall can consist of other materials besides brick, such as wood, steel and concrete blocks. The backup depends on the desired stiffness needed, for example concrete which is used to increase stability and rigidity of the wall diaphragm in multi-storey structures (Dizhur, Jiang et al. 2015). Following this presentation of the basics regarding the cavity wall system, the next section will demonstrate some relevant design updates concerning cavity wall construction and research on concrete blocks and metal wall ties testing throughout the 21st century.

In todays more modern cavity walls, the cavity widths measure around 100 mm which includes a typical air space of 25 mm and an insulation layer of approximately 75 mm in thickness. The insulation that can be used in walls can vary depending on thickness required and costs, with some examples of insulation consisting of polyurethane, polystyrene and rock wool. Insulation can be applied into the cavity wall in different forms such as using rigid board insulation or spray foams. Each insulation type has their own thermal resistances and advantages, although depending on the desired thickness, air space needed and overall cavity wall requirements, a cost-benefit optimization analysis needs to be performed for these structures. Insulation effectively retains heat during winter and minimizes heat gain in summer, resulting in lower energy costs, allowing for a potential future return on investment by employing insulation. The insulation reduces risk of moisture related damages like condensation and mold in walls. Another benefit of insulation can be reducing the need for heating and cooling, which not only decreases the cost for property owner's, but also lowers the building's energy demand and carbon footprint, contributing to a more sustainable environment (Al-Sanea, Zedan et al. 2003). A sample modern cavity wall is represented in Figure 1.3 with yellow foam insulation and brick veneer as exterior wall and concrete blocks as the loadbearing interior wall and another cavity wall showing the side view with the wall connecting metal ties.

Figure 1.3. Modern cavity wall system (Sigva 2018 and Mahajan 2021)

The exterior brick veneer has weep holes located at the bottom of the walls (above the foundation) which are gaps in between bricks not filled with mortar. These holes seen in Figure 1.4 allow for any potential water or moisture collected in between the walls from cracks in bricks or mortar to escape the cavity wall. These holes also allow for ventilation of air in and out of the cavity, promoting drying of the cavity and avoid moisture related issues (Potts 2022). The loading applied on these cavity walls occurs through the transfer of wind and seismic loads from the brick veneer through the ties and onto the loadbearing element of the cavity wall. Additional loads applied can depend on the temperature and moisture changes associated with the material used in the cavity walls which can vary at different rates. This allows for differential movement between the two walls demonstrating the importance of the components used such as the metal ties which will affect the structural resistance and stiffness of a building (DiDomizio, Quintana-Morales et al. 2024).

Figure 1.4. Weep holes in brick veneers (Schendelpest 2020)

Given the increasing impacts of climate change leading to greater temperature variations across the globe, the demand for enhanced wall insulation is rising and is expected to keep growing. Cavity widths are anticipated to exceed the typical 100 mm that were common 40 years ago to accommodate for more insulation in walls. Further research in this under-explored area is essential to explore the effect of larger cavities on cavity wall components such as concrete blocks and metal ties. (Hatzinikolas and Warwaruk 1991).

1.2 Intro hollow concrete masonry overview

Following the introduction of Portland cement, the use of concrete hollow blocks as the structural backing of a cavity wall became more in demand due to its greater performance capability as compared to individual bricks. This thesis investigates the compressive strength of hollow concrete masonry block assemblies under uniaxial monotonic compression loading. Concrete block masonry can be categorized based on its dimensions, mechanical and physical properties such that the blocks can be assembled using hollow, solid or hollow with grout. The hollow concrete blocks are found to be much less brittle and have a higher compressive strength than grouted blocks. Several reasons contribute to the lower compressive strength of grouted masonry. These include the presence of gaps caused by inadequate grout compaction and the creation of small cracks from the initial tension resulting from the shrinkage of the grout drying process. The masonry grouted assembly (prism) strength is around 80% of the hollow concrete masonry prism strength. The reason for the brittleness associated with grouted masonry is due to the mismatch in stress-strain characteristics between the grout and the concrete block which can generate lateral forces on the block and lead to premature system failure. Moreover, the tapered shape of the face shells and webs can cause the grout to act as a wedge as the grout wants to push outward from within the block, further contributing to early and brittle masonry failure and can be represented in Figure 1.5 (Fortes, Parsekian et al. 2015).

Figure 1.5. Compressive failure of a) hollow concrete masonry and b) grouted concrete masonry 2-course assemblies (Fortes, Parsekian et al. 2015)

A key design factor for engineers is the compressive strength of both the individual blocks and the mortared masonry assembly of the loadbearing CMU's. The CSA Group, specifically the standard of CSA S304-14, provides guidelines for testing the compressive strength of concrete block masonry, including strength and reduction factors that consider the height-to-thickness ratio of masonry specimens. These factors are considered conservative since they are based on substantial data of varying block dimensions and strength. The factors help simplify and reduce the costs and times of testing specimens since smaller mortared masonry specimens are easier to handle (Rizaee, Hagel et al. 2016). Research led by Drysdale and Hamid, who tested 146 concrete block prisms, found that masonry block specimens measuring 2-courses in height do not accurately represent the strength of concrete masonry since there was a reduction in prism compressive strength with an increase in prism height (Drysdale and Hamid 1979). This is why laboratory research on this topic and the CSA guidelines of recent years choose a larger height to thickness specimen such as testing of at least 5-course high masonry assemblies to better represent the characteristic compressive strength for masonry design and testing. Other research work highlighted how the height-to-thickness ratio and face-shell mortar bedding influence compressive strength. The face shell is the net area of the concrete block excluding the webs of the block in which the mortar is placed to join the next block to continually increase the height of the specimen (Figure 1.6). Several tests have demonstrated the impact of mortar strength and type with stronger mortar generally results in fewer lateral tensile cracks, which are the primary failure mechanism in prisms (Pasquantonio, PARSEKIAN et al. 2020).

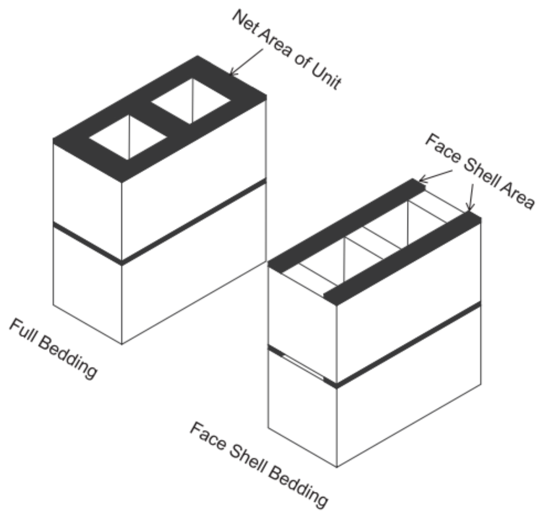

Figure 1.6. Mortar applied areas along the hollow concrete blocks (Sarhat and Sherwood 2014)

These studies among others contributed to the experimental testing procedure including compressive strength values and correction factors now included in modern CSA guidelines (Rizaee, Hagel et al. 2016). Drysdale and Hamid also observed that prisms made with blocks of relatively higher compressive strength tend to experience vertical cracking in the webs, particularly with face-shell mortar bedding. The solid part of blocks has a limited effect on the compressive strength of hollow prisms. Further research by Hamid and Chukwunenye determined that block size and mortar type have minimal impact on the elastic behavior of the prisms. Multiple studies have shown a correlation between higher compressive strength of blocks and higher compressive strength of prisms within a standard range of 10-30 MPa (Hamid and Chukwunenye 1986)**.**

Additional research has demonstrated that face-shell bedding results in higher compressive strength compared to full bedding which is mortar applied to the net area of the face including the webs of the block (Drysdale and Hamid 1979). The CSA mandates the testing of running bond prisms which can represent compression testing and suggests that stack pattern may be used to represent other bond types. The running bond pattern in a masonry assembly allows for two half blocks to be connected by a vertical joint for every second mortared block along the height of a mortared prism, while a stack pattern consists of full blocks mortared one on top of the other along the specimen height (Figure 1.7). However, it was found that the presence of a vertical joint in a 3-course high running bond pattern of caused a notable decrease in the strength of the prism. This preliminary result of strength loss is likely because the block's face shell and webs are not aligned and do not match up with the block's transverse walls (Mohamad, Lourenço et al. 2011). With numerous tests and research concerning compressive strength of concrete masonry, there are some shortcomings that will be discussed in section 1.4.

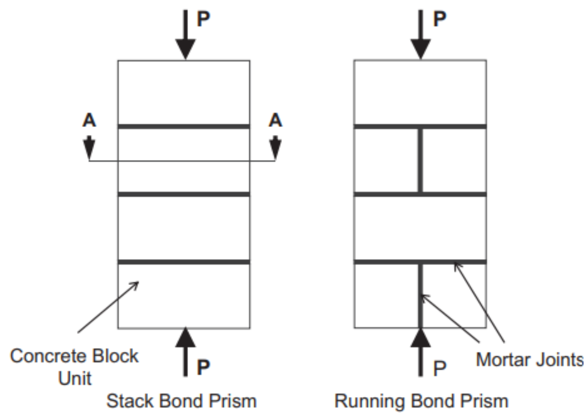

Figure 1.7. Types of mortar bond patterns for masonry concrete block construction (Sarhat and Sherwood 2014)

1.3 Metal cavity wall ties overview

Another element from the masonry cavity wall design that will be studied in this paper are the metal cavity wall ties which connect the brick veneer to the concrete block wall by embedding them in between the mortar of concrete block structural backup and brick veneer mortar. These tie types are called block connectors while another type of tie being explored in this thesis is the slotted rap tie which would be drilled into wood or steel studs acting as the loadbearing backup and connected to brick veneer through a tie clip (V-tie). These types of ties analyzed in this thesis are similar to the ones analyzed in a paper from Ismaiel, Chen et al. concerning their thermal rather than their mechanical properties (Figure 1.8). These ties are considered adjustable ties since they have an adjustable slot that allow the clips to embed in the brick veneer mortar and accommodate shifts in position during installation or loading of the ties in the wall. There is limited research data performed on these types of ties as compared to the many more studies on older and non-adjustable design of ties. These ties can take different forms of thin pieces of metal wires, rods, and corrugated strip ties to name a few and can be observed in Figure 1.9 (Martins, Vasconcelos et al. 2017).

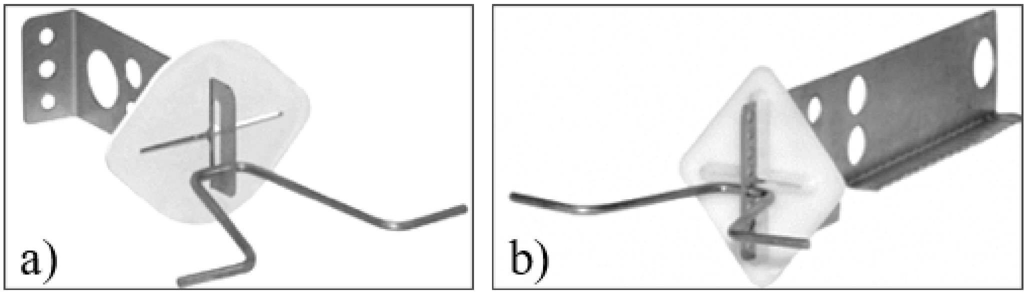

Figure 1.8. a) slotted rap tie b) block connector (Ismaiel, Chen et al. 2022)

According to modern standards from CSA A370, the maximum allowable spacing of ties in a cavity wall is 800 mm horizontally and 600 mm vertically, resulting in a load-bearing area of 0.48 m^2 for each tie. The maximum cavity width although not necessarily reached in structures is 150 mm in thickness. The following section will show the past and relatively modern tie testing in literature.

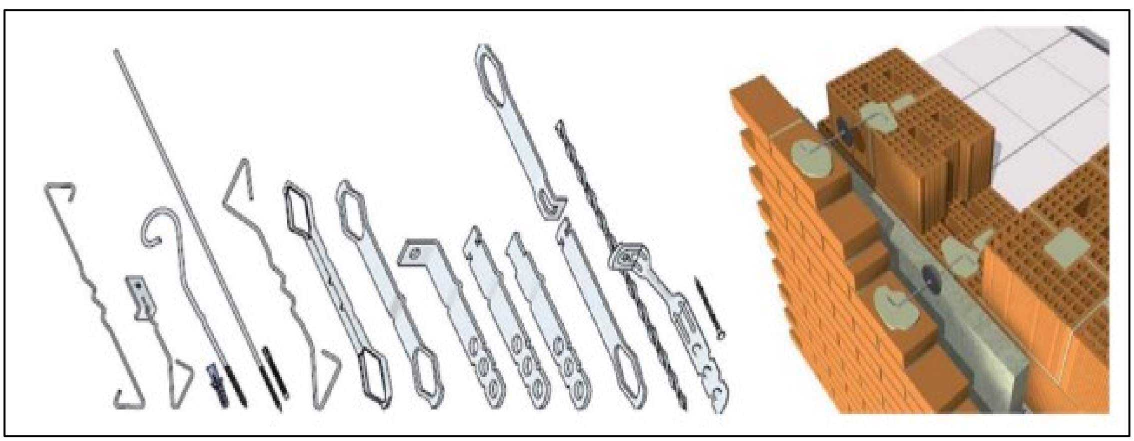

Figure 1.9. Numerous types of ties and sample tie embedment in cavity wall (Martins, Vasconcelos et al. 2017)

The pioneering research in cavity wall ties testing was performed by Hatzinoklas et al. and the experimental setup can be found in Figure 1.10. This setup was the basis for various studies which utilized a hydraulic jack that can apply pressure to the cavity wall for both tension and compression to study the tie connection load resistance of the ties and therefore the performance of the overall small cavity wall system (Hatzinikolas, Longworth et al. 1983). The polystyrene layer in the compression setup acts as a sponge and allows the jack to continually compress the specimen as it moves along on the plate until failure. For the tension test, the brick veneer is restricted from moving along the track with the plate as its being pulled away by the concrete blocks by the jack operating in the opposite direction. In the compression test, the opposite occurs as the jack pushes the concrete blocks rather than pull them along the track.

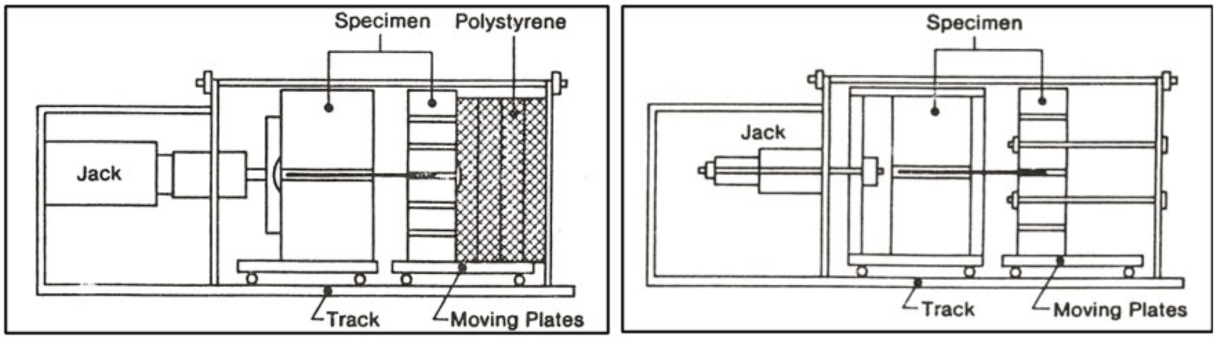

Figure 1.10. Small cavity wall system setup for compression (left) and tension (right) testing (Hatzinikolas, Longworth et al. 1983)

The study performed by Hatzinokolas et al. provides a substantial analysis of tie testing in small scale cavity walls, albeit with much thinner steel ties with low load resistances and for around 100 mm thick cavity walls with respect to the codes and standards of that era. The paper performed a total of 66 tests on adjustable ties that embed into the mortar of concrete block backing and adjustable wire ties (‘T’ ties) that are fastened through insulation layer to a metal stud loadbearing support using a screw (Figure 1.11). It was found that the adjustable ties had an average peak load in compression of 1.55 kN, while it had an average peak tension load of 2.23 kN. Of the recorded failures, 20% occur within the adjustable ties across both tension and compression tests. A noticeable point upon reviewing the test data reveals that the peak load resistance decreases with longer metal ties in larger cavity width walls which demonstrates buckling of metal ties with longer sizes. As for the ‘T’ ties, 18 compression tests were performed with 80% of failures occurring by buckling of the tie and damage to steel stud with an average peak load of 2.66 kN. While for tension, almost all the 39 ‘T’ ties specimens failed with the fastener screw being pulled out of the stud at varying peak loads and this was attributed to the position of the fastener screw with respect to the embedment of the tie in the veneer brick and the strength/thickness of steel stud (Hatzinikolas, Longworth et al. 1983)

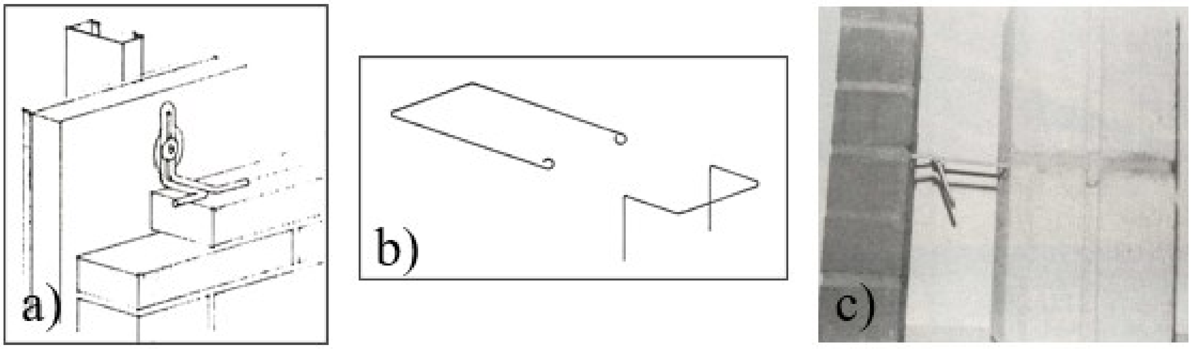

Figure 1.11. a) T ties setup in cavity wall b) adjustable tie c) adjustable tie embeded in cavity wall (Hatzinikolas, Longworth et al. 1983)

Among the only studies that have similar tested block connector ties to those being analyzed in this thesis come from Williams and Hamid as seen in Figure 1.12 (Williams and Hamid 2005). The experimental testing consisted of three ties, however the two types of ties related to this thesis are the two ties with varying adjustable slot types to accommodate for the position of V-tie clip embedment in brick veneers. The tie type designated as type T2 allows for both vertical and horizontal in-plane movement, while type T3 has holes as the connecting slot which only allows for horizontal in plane movement of the veneer.

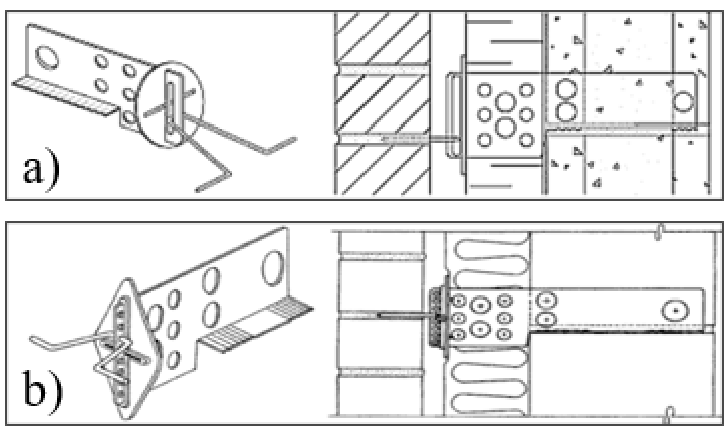

Figure 1.12. Block connectors a) T2 with large adjustable slot and b) T3 with hole adjustable slot (Williams and Hamid 2005)

Also, it is noted that the tie specimens were tested in a small cavity wall assembly, rotated to orient the V-tie clips for vertical loading between two bricks, rather than the conventional method of embedding the clips horizontally in the stacked mortar joints of the brick veneer as depicted earlier in Figure 1.11a). To measure the differential displacement between the back-up wall and the veneer, the brick veneer masonry was subjected to a force from a loading machine while the two mortared concrete blocks were kept stationary. The orientation and experimental setup of this are shown in Figure 1.13 This setup applied a compressive load parallel to the mortar joint, creating a bending effect along the adjustable slot of the ties due to differential loading, rather than the typical uniaxial tension and compression transfer of force used as the loading protocol of this present thesis.

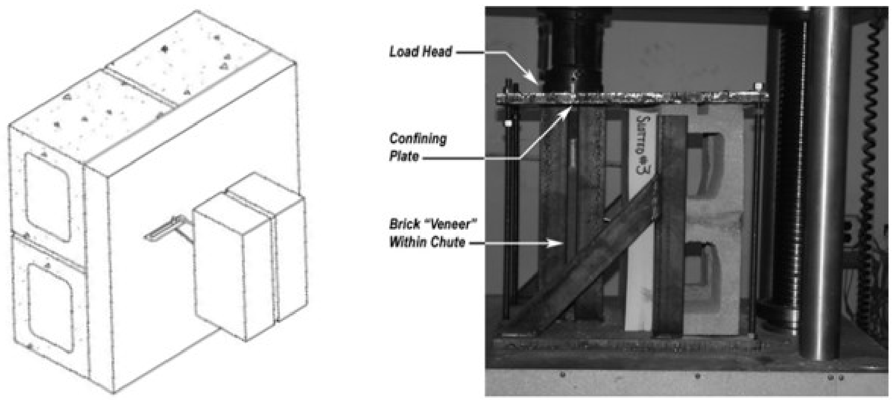

Figure 1.13. Small cavity wall orientation with test setup (Williams and Hamid 2005)

These ties have holes to allow for better energy efficiency in structures. Since metal ties connect the loadbearing structural part and the outer veneer part of the structure, they can create thermal bridges through the insulation. The thermal resistance of a material is its ability to resist heat flow; the higher the thermal resistance (R-value), the better it is at insulating structures. To improve energy efficiency and minimize heat change, it's important to use wall ties that have higher thermal resistance, often achieved by incorporating thermal breaks such as gaps/holes in steel since air is a weak conductor of heat as compared to metals or other solid materials. These measures help minimize thermal bridging and maintain the insulating integrity of the cavity wall system. It is noted that having holes in ties as compared to without holes increases the thermal resistance of the ties about 5% and that stainless steel has a higher R-value than galvanized steel. These holes contribute to thermal benefits as they also allow for decreased steel usage and therefore create more sustainable design practices (Ismaiel, Chen et al. 2022).

With comparing the testing of the T2 and T3 ties, the average peak load for the T2 ties was 2.6 kN with a stiffness of 0.17 kN/mm while the T3 was 2.33 kN with a stiffness of 0.12 kN/mm. The study does not provide relevant dimensions and positioning of the ties nor the standard deviation of loads and stiffnesses of the tested samples. As can be seen in Figure 1.14, these tie types have diverse failure modes : the T2 type underwent a twisting action in the adjustable slot as the tie was continuously laterally loaded, whereas the T3 tie, which has its V-tie clip connected to holes rather than a full adjustable slot, was bending but not deforming along the slots (Williams and Hamid 2005).

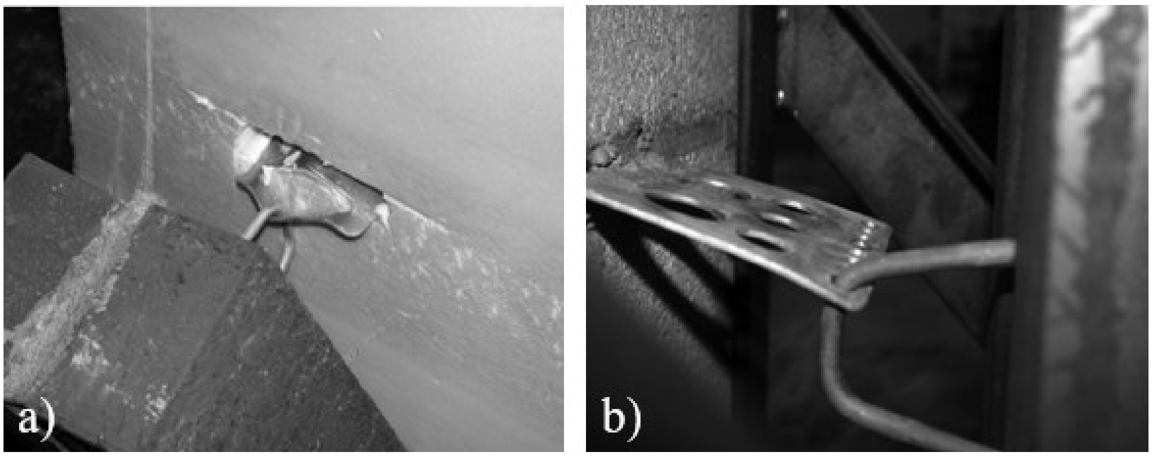

Figure 1.14. Failures associated with lateral applied load on a) T2 ties and b) T3 ties (Williams and Hamid 2005)

1.4 Knowledge gaps and scope of research objectives

The literature in past research acknowledges that both the height-to-thickness ratio and bond pattern influence the compressive strength of concrete masonry prisms. However, few studies have examined how these two combined factors interact. The CSA S304-14 standard requires testing of running bond samples to determine masonry compressive strength, but this process is complex and rarely performed in labs. This study will test numerous specimens of varying heights to further our understanding of the underlying relationship between strength, modulus of elasticity, failure mode and size effect, under uniaxial monotonic compression, as stated in CSA S304 which examines design of masonry structures. The specimens to be tested include single course blocks, 2-course (doublets), 3-course (triplets), and five-course mortared prisms (will be referenced as ‘HJ and VJ prisms’ in results section). The triplet and 5-course prisms are constructed in both stack bond (horizontal joint: HJ) and running bond pattern (vertical joint: VJ).

The novelty of testing the concrete masonry assemblies in both running and stack pattern bond is to create a relationship between the size effect of the specimens and the constructed bond pattern of these specimens. These experimental tests will be compared to the strength correction factors found in CSA S304-14 which allow for theoretically finding the strength of a specific height of concrete masonry specimen (Figure 1.15). However, if the experimentally determined strength values are unrepresentative of the correction values found in CSA, adjustment to the CSA guidelines may be necessary. The CSA continuously performs and analyzes research to update their standards consisting of clauses and tabulated results in which this research can provide further insight into future guidelines in creating more compressive strength data tailored to specific types and dimensions of concrete blocks.

Table D.1
Correction factors
(See Clauses D.3.2.3, D.5, and D.6.5.)

Height-to-thickness ratio*	Correction factor
2	0.85
3	0.90
4	0.95
5 to 10	1.00

*Linear interpolation may be used.

Figure 1.15. Table D.1 Correction factors depending on compressive strength data from CSA

Despite numerous tests on other types of ties, there are few tests performed on modern adjustable ties (Hatzinikolas, Longworth et al. 1982). The available and dated research does not include the load resistance over a large range of modern adjustable tie sizes, especially for ties that accommodate a cavity wall significantly greater than 100 mm in thickness. The impact on load resistance and stiffness of ties due to eccentric loading along the adjustable slot of ties is also scarce**.** For adjustable ties, CSA A370-14 suggests testing the ties in at least two positions along the adjustable slot, however limited and insubstantial research is available on these types of ties and loaded in eccentric positions. The eccentric loading of ties is mentioned in CSA A370, yet it is a side note and not much information regarding its applied impact on tie strength and stiffness in a cavity wall system (Williams and Hamid 2005). The eccentric loads occur with the possible misalignment of tie components due to variations in the heights of masonry courses, as well as differences in the foundations that may affect the height between the two walls in the cavity. The adjustable slot allows the tie clip to shift, embedding it in the available and corresponding brick veneer mortar at an eccentric position. Additionally, errors during installation and long-term differential movements could also cause misalignment, depending on the tie design. Given the need for wider cavities to mitigate the predicted variations in temperatures due to climate change by inserting more insulation, it is unclear how longer ties will be effective in providing the necessary strength connection between cavity walls for this durability challenge.

Additionally, with more insulation space in the cavity walls, the longer ties need to be able to respect thermal resistance requirements for structures and having less ties in a specified area of the wall can help, but it remains to be seen if longer spans between ties can withstand environmental loads. With potential for making and utilizing stronger ties, having less ties within specific areas of walls can respect thermal resistance (R-value) needs of structures and create more sustainable construction practices (Sparling, Palermo et al. 2021). To create a substantial data record of the modern adjustable tie testing for both load resistances and stiffness, the ties studied in this paper are tested as individual specimens in a specially designed setup, rather than mortared in between a concrete block doublet setup or connected in a small cavity wall system as seem in the past literature research (Skroumpelou, Messali et al. 2018). The level of experimental testing on ties in this paper is unprecedented due to the numerous tests on varying lengths and types of ties along the centric and eccentric loading positions. The ties are tested in both compression and tension. This paper accounts for a large variation of insulation thicknesses in the cavity walls and the types of steel ties involve both hot-dip galvanized (HDG) and stainless steel (SS) types.

According to the CSA A370-14 guidelines, there is little information on expected load resistance and stiffness of ties since there are numerous types available depending on various construction requirements. The tie specifications provided from the companies of BLOK-LOK and FERO being studied in this research only provide a general peak load resistance for the ties, however, they don’t provide the necessary info for each tie size and the effect of eccentric loads and stiffness of the ties. The testing of individual modern cavity wall ties may suggest a need to establish new standards to show potential resistances and governing failures based on tie types, lengths and load positioning to optimize construction techniques tailored to their specifications.

This research examines the essential components of masonry cavity wall systems, specifically the compression testing of concrete masonry assemblies and cavity wall ties. The objective is to offer insights that contribute to updating standards and industry-regulated structural elements, ultimately improving the sustainability and performance of masonry construction.

2 Experimental testing

This experimental campaign includes over 50 compression tests of concrete hollow block assemblies ranging from 2, 3 and 5 courses in height for both stack and running bond patterns. Additionally, there are 240 tests equally distributed between compression and tension tests. These tie tests were independently tested rather than in a cavity wall assembly. The ties tested measured from 3” to 8” designated insulation thicknesses for BLOK-LOK ties and three tie dimensions in the range of 54 mm to 155 mm tie lengths for the FERO ties. The testing of BLOK-LOK ties involves three loading positions along its adjustable slot, while the FERO ties were tested in two positions. This section will investigate the material properties, procedures, test setup design and assumptions taken associated with the testing of the concrete and metal wall ties specimens.

2.1 Concrete block and mortar used to cast and test over the research campaign

The concrete blocks used in the research were manufactured by Groupe MBM with design specifications of 191.4 x 389.7 x 195.6 mm and commonly referred to as 20 x 40 x 20 cm long stretcher blocks. These hollow blocks are fabricated in accordance with CSA A165. The blocks have a gross net area of approximately 46 800 mm^2 and a face shell bedding area in which mortar is typically placed to stack blocks has an average of 36 500 mm^2. According to Groupe MBM, an individual block can withstand a 1250 kN compressive force which translates to a compressive strength of approximately 26.7 MPa.

Figure 2.1. Hollow concrete block and Type S mortar used in specimen casting

The mortar used to bond the hollow concrete blocks together is of Type S from the company King Block and is designated with an ‘S’ to be used in structural loading applications, rather than non-loadbearing uses like other mortars such as Type N on exterior veneer walls.

A total of twenty-seven type S mortar cubes, each measuring 50x50x50 mm were prepared in metal cube molds and left to cure for 28 days before subjecting them to compression testing. The mortar cubes were tested in uniaxial compression using an MTS Rock Frame machine, with a capacity of 4600 kN and the mortar was tested following the loading protocol outlined in CSA A179-14, which involves a force-controlled loading approach. A loading rate of 0.008 mm/s was used, and the test was concluded when a drop of more than 5% from the peak load was observed.

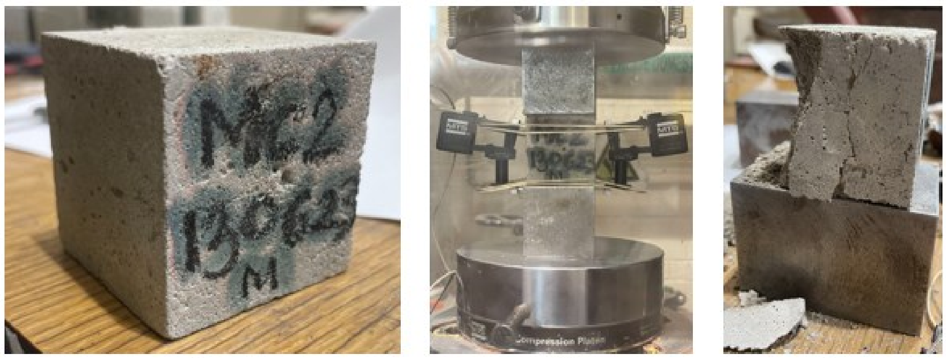

a) b) c)

Figure 2.2. (a) Mortar cube (b) mortar cube in Rock Frame machine test setup with extensometers (c) compression failure of mortar cube

The mortar cubes were also fitted with 50 mm-gauge length extensometers using elastics to hold them in position for the purpose of detecting more precise deformation measurements to measure strain and obtain the modulus of elasticity of the mortar (Figure 2.2). The mortar's average compressive strength was found to be 22 MPa, while the modulus was 6436.16 MPa. A sample of the tested data had the stress versus strain relationship presented in Figure 2.3.

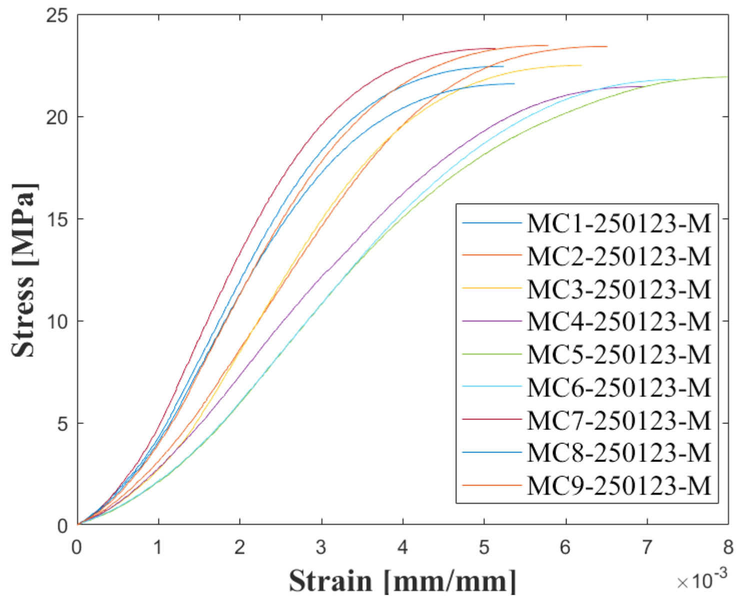

Figure 2.3. Stress vs strain relationship for compression testing of mortar cubes

2.1.1 Concrete block assembly casting process

The process of casting and creating concrete masonry block assemblies involves various machines, techniques and training. Utilizing the mortar preparation guidelines in CSA A179, the mix proportion and workability were respected, assuring proper use for the mortar. The mortar was made using a large mixing machine which mixed the contents of mortar and water to create the ideal and workable mortar to bond the concrete blocks together. The mortar is applied to the concrete block in the face shell bedding area as can be seen in the (Figure 2.4a) using a wood formwork. To add the correct amount of mortar to the area of the block, a wood mould with cut out pieces to accommodate the face shell area was added to the top of the block. The wood form measuring a little more than 10 mm in thickness was placed over the block and the desired mortar was applied to the block to achieve 10 mm mortar joints (Figure 2.4b). As the next block was stacked onto the face shell mortared bed, pressed and levelled into the mortar to create proper bond, any excess mortar was removed and before the mortar hardens, the mortar joints were tooled. This was performed by pressing a metallic curved rod onto the joints which slightly compressed the mortar in the joints and provided a smooth finish (Figure 2.4c).

After all necessary specimens were casted, the samples were covered with a polyethylene sheet to create an enclosed chamber for 7 days under the sheet (Figure 2.4d). From day 7 to 28, after specimen casting, a humidifier was used to regulate the humidity in the chamber to respect the

CSA S304-14 range of 30-70% relative humidity for the continuous curing and strengthening of the mortar bonds. The average relative humidity over the curing period was found to have an average of 60% using humidity sensing battery powered monitors which were placed at various positions surrounding the mortared blocks in the enclosed plastic chamber. After the curing period of 28 days, the casted specimens were ready to undergo compression testing. Similar casting procedures for both stack and running bond patterns, with the exemption of a vertical mortar joint that should join two half blocks together for the running bond specimens, for every second mortared block along the specimen height.

Figure 2.4. a) Face shell bedding area of mortar on block b) wood mould to apply 10 mm mortar joint c) complete specimen construction d) plastic sheet covering casted specimens

2.1.2 Compression testing setup for masonry specimens

The compression testing of the concrete block masonry was performed using a 12 mega newton (MN) MTS machine capable of performing monotonic uniaxial compression loading and allows for required load rate application on specimens as per CSA S304-14 clause D.4.5. The MTS machine can measure force (kN) and displacement of the load head (mm). As per the specification, the load application is divided into two segments: the first rate applies half of the expected maximum load reached, and the second loading rate applies the remaining load at a uniform rate within 1 to 2 minutes. After running some initial tests on various sized masonry assemblies, the optimal rates were a loading rate of 250 kN/min during the first segment until reaching 500 kN, followed by a strain rate of 0.2 mm/min per number of individual blocks in the tested specimen, which means that for a 5-course concrete prism assembly, the strain rate would be 1 mm/min. As can be seen in Figure 2.5, the masonry specimens are capped with 30 mm thick steel S-grade plates using a white gypsum (Hydro-Stone gypsum cement) to bond the concrete and steel together. The steel plates allow for uniformly distributed pressure on the masonry block specimens (CSA S304-14). Due to the size and weight of the specimens, a forklift was used for lifting and centering the concrete specimens on the steel base plate where the MTS load actuator compressed the samples. The specimens were also fitted with four linear variable differential transformers (LVDT), two on each longitudinal side of the block which each have +/- 15 mm of accuracy. The LVDT's were placed at the quarter points from the ends of the block and they stretch over one mortar joint for doublets, while the LVDT's stretched over two mortar joints for triplets and 5-course assemblies. The LVDT gauge length for the doublets was 200 mm, while for triplets and the 5-course prisms the length was 400 mm to account for two mortar joints and to have a better collection of data across larger specimens. These devices are removed when the MTS machine is paused to transition from force-based loading to displacement control for the well-being of the LVDT's in the event of extreme or explosive compression block failure. These sensors allow for strain measurements (mm/mm) and obtaining the modulus of elasticity of the specimens which is the initial slope of a stress (MPa) versus the strain graph within the range of 5-33% of the peak strength (CSA S304-14). The modulus of elasticity is a measurement which checks an objects resistance to deformation and therefore a high value of modulus of elasticity signifies minimal deformation under applied load.

Figure 2.5. Setup for the concrete masonry assemblies in the MTS machine

2.2 Ties overview

The ties testing involves two types from BLOK-LOK and FERO and are called BL-507 veneer anchor and FERO Thermal tie – slotted rap tie masonry connector (Figure 2.6). The BLOK-LOK ties are used in cavity walls by embedding into the mortar of loadbearing concrete blocks and the triangular FLEX-O-LOK clip which attaches to the adjustable slot on the tie and embeds in the brick veneer mortar. The FLEX-O-LOK clip is a hot-dip galvanized (HDG) steel with a diameter of 80 mm and thickness of 6 mm. This clip can move along the adjustable slotted opening measuring 50 mm in length with a height of 7 mm.

While for the FERO ties, these types also have clips called V-ties which embed into the brick veneer, however they differ from the BLOK-LOK ties since these ties are screwed into structural backing of wood or steel, rather than embedded in mortar between concrete blocks. The V-tie clips from FERO are available in a variety of sizes such as the 60 mm in length which were tested with the smaller ties of 54 mm and 105 mm in length, while the 80 mm V-tie clips were tested with the 155 mm ties. These FERO ties are also tested in HDG and stainless steel (SS). The hot-dip galvanized V-ties have a thickness of 6 mm, while the stainless steel (SS) have slightly smaller thickness with of around 5 mm. The HDG clips have a more roughly finished surface contrary to the SS ties which are very smooth.

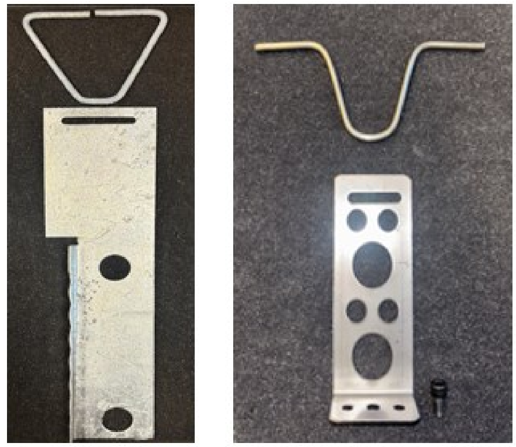

Figure 2.6. BLOK-LOK tie with FLEX-O-LOK clip (left) and FERO tie with V-tie clip (right)

The way the ties from BLOK-LOK and FERO denote the length of their ties can be found in Figure 2.7. They are designated by the typical length of insulation these ties can cover and therefore do not represent the entire width of the cavity wall. The lengths of the ties specified by BLOK-LOK and FERO will be used in the results and discussion section. The cavity widths of the walls would be the length specified by the tie manufacturer plus about 2 inches to account for the adjustable slot spacing and about a 25 mm air space in between the tie and outer brick veneer wall.

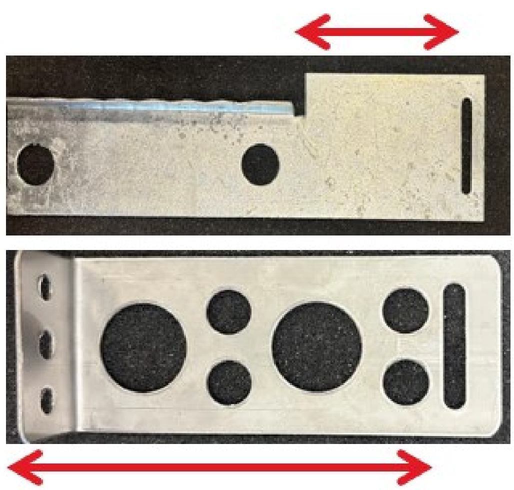

Figure 2.7. Length of tie values specified by BLOK-LOK and FERO

A total of 240 tests were conducted using both types of ties, equally divided between tension and compression tests. Each tie length and loading position of both companies were tested using 10 ties: five were tested under compression and the other five under tension to allow for representative results and following CSA A370-14. Depending on the location where the tie clips embedded into the mortar in brick veneers, centric loading conditions did not necessarily align along the slot. The tie clips sometimes required an adjustment to accommodate for the embedment in the brick veneer mortar and therefore the loading on the ties may be applied in an eccentric way along the adjustable slot, creating a moment in the metal tie. To evaluate the eccentric loading effect on the ties, the BLOK-LOK ties were tested in the middle of the slot as well as the extremities of the open slot (left and right positions). In comparison due to a more symmetric structure of tie, the FERO ties were tested in the middle and only in the left-most position of the slot. The notations for interpreting the positions of the clip in the adjustable slot were designated as ‘M’ for middle, ‘L’ for left and ‘R’ for right side of the slot. This configuration can is depicted in Figure 2.8.

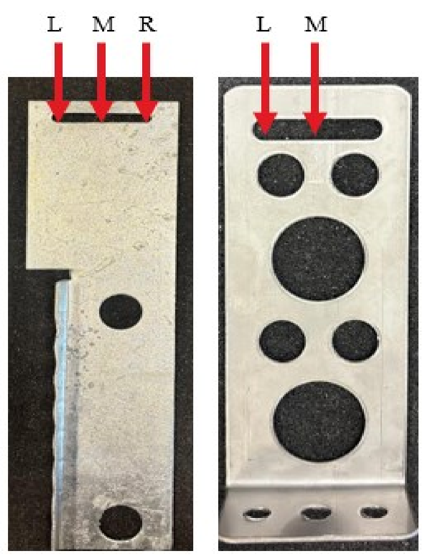

Figure 2.8. FLEX-O-LOK loaded positions along slot (left) and FERO loaded positions along slot (right)

The machine that can apply the loads and accommodate the test setup is an MTS Sintech 30/G with a load capacity of 150 kN as seen in Figure 2.9. The machine can record the applied force versus displacement of the load head. An LVDT like the one for the compression testing of masonry blocks was used, however the accuracy parameter was set at +/- 30 mm to check the displacement measurements of the machine.

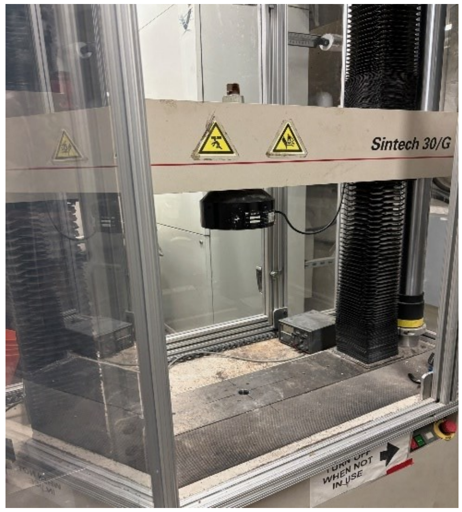

Figure 2.9. MTS Sintech 30/G machine

Some relevant information on testing of these cavity wall ties can be found in clause 12.1 of CSA A370-14 which include load rates and mechanical free play. The load rates of the specimens were found through the process of trial and error to respect that the maximum load should occur in the range of 1-2 minutes. As for the mechanical free play, it is necessary to allow for the accommodation of differential movement between the inner and outer leaves of a cavity wall to prevent direct transfer of stresses between the two walls while preserving the wall's initial integrity. The free play contributes to the wall's long-term durability by reducing the risk of premature failure in the ties or masonry elements. With the ability to allow for slight movements before activating the tie strength and stiffness, the ties can absorb and dissipate stresses over time. This decreases the chances of early fatigue on the ties and the connecting mortar which results in extending the wall's lifespan. During testing, the tie clips were positioned to allow a small gap between the top and bottom part of the adjustable slot opening, this allowed for free play preventing the clip to touch either side of the slot on the tie.

The ultimate force or strength of the ties was found by applying certain factors which make the tie strength conservative. These factors may depend on the failure mechanism in the tie, the tie embedment and the coefficient of variation (COV) of the tested ties. As per CSA A370, the peak load of the tie should be the greater of the force reached before or at 4 mm of displacement for both tension and compression (Figure 2.10). A factor of 0.9 is multiplied to the peak load in the event of failure of the tie such as buckling or cracking, while a factor of 0.6 is applied to the peak load in the event of embedment failure (due to mortar, brick or concrete failure). The embedment failure factor will not be applied to the ultimate strength calculation of the ties since this research campaign does not investigate the tie embedment in mortar, but rather the 0.9 factor will be applied for the tie breaking in tension and buckling in compression. Another factor to be applied to the peak load consists of (1-1.64(COV)) with the chosen COV being the greater COV of the tested ties or 10%.

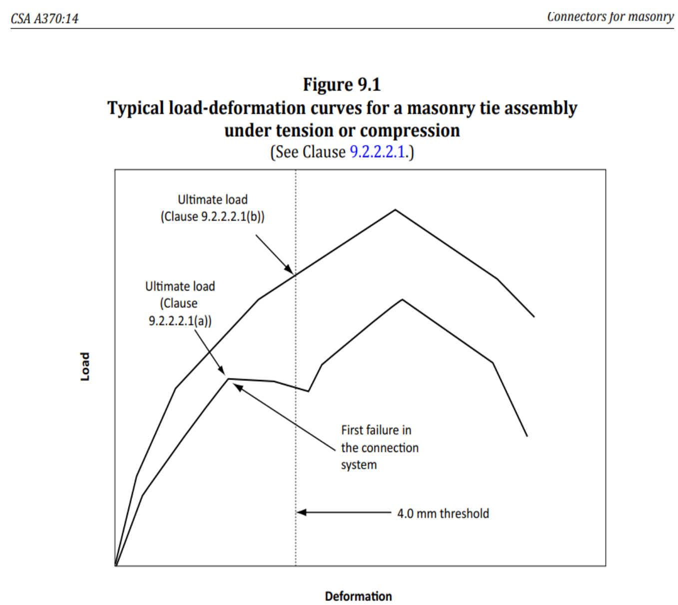

Figure 2.10. Peak load selection criteria based on load-deformation curves (CSA S304-14)

The stiffness of ties is not a mandatory part of CSA guidelines; however, knowing the stiffness of ties can be beneficial in having a better understanding of their contribution to the overall stiffness of masonry wall cavities. A less stiff and more flexible tie may not be adequate in transferring loads from wind and seismic forces, which leads to structural issues. The same can be assumed for stiffer ties which may cause further stresses within the ties and transfer loading onto surrounding masonry components which may cause premature failures as well. Since there are no available procedures in finding stiffness of ties, the stiffness was calculated following the same range as the modulus of elasticity of the masonry compression tests. The slope of the force (kN) vs displacement (mm) graph in the range of 5-33% of the tie peak load was used to find the tie stiffness.

2.2.1 Test setup and relevant information for BLOK-LOK ties

These types of ties are much wider and longer than those from FERO and created a challenge in accommodating a test setup. After evaluating various ideas and designs, an optimal setup was created in the lab using steel blocks capable of withstanding the forces reached in the testing of metal ties. Since the ties were tested independently rather than within concrete blocks or a cavity wall system, many more tests were conducted to measure their strength and stiffness under individual tie tests in compression and tension. To simulate the ties as they would be embedded in a cavity wall, the testing setup included a top steel block attached to the machine's load head which allowed for load translation to the tie as presented in Figure 2.11. The FLEX-O-LOK clip was inserted into a grooved small steel block, allowing the clip to rest securely in the grooved area. The clip was then clamped in between the grooved block and the larger steel block connected to the machine using screws. This setup mimics the way the clip would be embedded in the mortar between two veneer bricks. The part of the clip not clamped extended out of the steel block, creating a "cavity" connection to the rest of the tie.

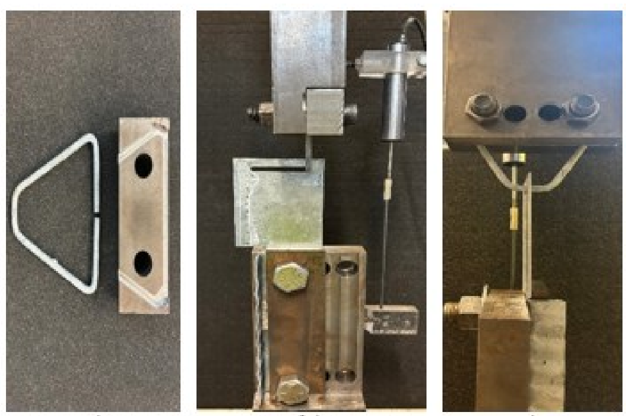

a) b) c)

Figure 2.11. a) FLEX-O-LOK clip with grooved steel block b) front view BLOK-LOK tie setup c) side view of BLOK-LOK setup

Similarly, the bottom of the tie with the corrugated part that would usually embed in the mortar along the web of concrete blocks was clamped in between a steel block and a steel plate using two 1-inch screws going through the holes in the bottom of the tie. These holes in the BLOK-LOK tie were designed to enhance mortar interlocking when embedded between concrete blocks, therefore clamping this corrugated region with steel closely simulates its actual use in masonry. Although this setup doesn't replicate all the materialistic components of a cavity wall system, it effectively measures the strength and stiffness of an individual pin-fixed tie. The holes of the 8” length BLOK-

LOK tie had its top hole located closer to its bottom hole and therefore an extra set of holes were needed to be drilled through the steel setup. Also, to account for eccentric testing of the BLOK-LOK ties, a total of 2 extra holes per row matching the holes in the ties were drilled in the steel bottom block setup. This allowed for positioning of the ties at the extremities of the adjustable slot. The Table 2.1 shows the convenient testing rates across the varying lengths with minimal fluctuation out of the desired time range (CSA A370-14).

Table 2.1. Load rates across tested BLOK-LOK tie lengths and load positions along the slot

BLOK-LOK ties	**8” -M**	**8” -L**	**8” -R**	**6”- M**	**6” -L**	**6” -R**	**5” -M**	**5” -L**	**5” -R**	**3” -M**	**3” -L**	**3” -R**
Tension rate mm/min	3.0	3.0	3.0	2.0	3.5	4.0	2.5	2.5	2.5	2.5	2.5	2.5
Compression rate mm/min	1.0	0.8	0.8	1.0	1.0	1.0	1.0	1.5	1.5	2.0	2.0	2.0

2.2.2 Test setup and relevant information for FERO ties

The FERO ties have a different connection to the loadbearing part of the structures as compared to the embedment into mortar of concrete blocks for BLOK-LOK ties. The FERO ties require a fastener to screw into a metal or wood stud backup, while its V-tie clip is like the FLEX-O-LOK clip of BLOK-LOK in which the clip embeds in the veneer mortar. The setup for the FERO ties can be seen in Figure 2.12 and consists of the same steel block that is screwed into the Sintech machine load head as the BLOK-LOK setup, however the block with the grooved area is different to accommodate the V-tie shape clip from FERO. These clips were inserted into the grooved block and clamped to the other steel block connected to the Sintech load head using screws to replicate the embedment in the mortar of brick veneer. As for the loadbearing connection, a steel block was used with three ¼” drilled holes to allow for eccentric loading of the ties, and a hex screw measuring ½” with a ¼” diameter fastened the tie to the steel block. This connection to the steel block represents a structural steel stud as a loadbearing backup to the cavity wall system.

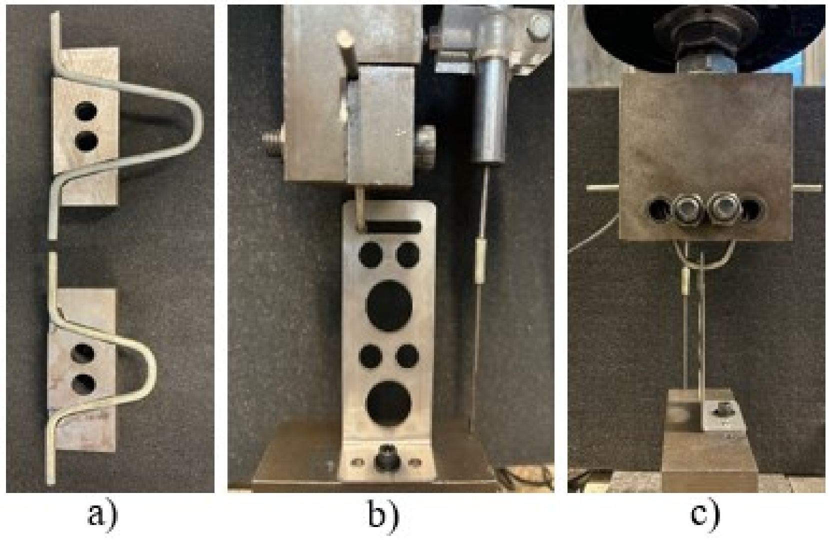

Figure 2.12. a) V-tie clips embedded in grooved steel blocks b) front view of FERO tie setup c) side view of FERO tie setup

The FERO ties were tested in the middle slot position and could have been tested on either the left or the right extremities of the slot, however only the left side of the adjustable slot was tested since these ties are symmetric with their circular gaps in the steel of the tie. The V-tie clip could move along the 35 mm adjustable slot having a height of 7 mm. The holes in the ties are for increasing the R-value to enhance the resistance to heat transfer through the ties and the overall cavity walls. Strategic placement of these holes allows for better insulation performance; however, it may affect the strength or stiffness of the ties as there's less steel material to carry loads. Just as with the BLOK-LOK ties, the mechanical free play was also performed on these ties. The load rates that effectively maintain the requested peak load within a 1–2-minute range are listed in Table 2.2 (CSA A370-14).

Table 2.2. Load rates across tested FERO tie lengths and load positions along slot

Type of ties	**HDG**		**SS**		**HDG**		**SS**		**HDG**		**SS**	
Tie lengths and position	**54 mm -M**	**54 mm -L**	**54 mm -M**	**54 mm -L**	**105 mm-M**	**105 mm -L**	**105 mm -M**	**105 mm -L**	**155 mm -M**	**155 mm -L**	**155 mm -M**	**155 mm -L**
Tension rate mm/min	6.0	6.0	5.0	5.0	6.0	6.0	6.0	6.0	6.0	6.0	5.0	6.0
Compression rates mm/min	3.0	1.0	2.0	1.0	1.0	1.0	0.8	0.8	1.0	0.8	1.0	0.8

3 Experimental results and discussion

In this section, the summary of both experimental results for the concrete masonry and metal ties testing will be discussed and presented using tables, graphs and illustrations. This will allow for a better understanding of the variations and comparisons that can be made across testing of all the specimens.

3.1 Compression test results of concrete masonry assemblies

Table 3.1. Compression test results of concrete masonry assemblies

Specimen	Peak force (kN)	Compressive strength (MPa)	COV %	Modulus of elasticity (MPa)	COV %
Single (9)	1250	26.7	7.2	-	-
Doublet (11)	980	26.8	6.8	23 670	10.4
HJ-triplet (13)	895	24.5	13.1	20 365	17.0
VJ-triplet (6)	765	21.0	11.6	17 350	16.2
HJ-prism (10)	840	23.0	12.8	17 700	11.0
VJ-prism (4)	750	20.5	10.0	15 750	7.6

The results of testing the compressive strength and modulus of elasticity of the concrete masonry can be found in Table 3.1. Some notations pertaining to the referenced table are that the stack pattern is designated as horizontal joints (HJ) and running bond pattern is designated with vertical joints (VJ). The number of tests performed on each specimen are found in brackets next to the names of the specimens in Table 3.1. The table and Figure 3.1 show that compressive strength and modulus of elasticity decreases as the height to thickness ratio of the concrete prisms increases. The single block compressive strength is very similar to that of the doublet strength due to the force being divided by a greater net area as compared to the face shell area for doublets which is smaller, however the single blocks can withstand a much higher peak load. As can be seen in Figure 3.1, the stack patterns had a compressive strength decrease of 9.5% and 6.5% for the doublet to triplets and the triplets to HJ-prisms, respectively. The compressive strength reduction for both the HJ-prism from a doublet and the VJ-triplet from a HJ-triplet are 15%, while the reduction of the VJ-prism from the HJ-prism is 10%. Using the LVDT's, the modulus of elasticity of the VJ-triplets was found to be 17% less than the HJ-triplets and the VJ-prism reduction from the HJ-prism was

12.4%. The elastic modulus of the doublet and HJ-triplet increased by 34% and 15%, respectively, compared to the HJ-prism. The VJ-prism had a 10% reduction in modulus from the VJ-triplet value. This shows that the bond pattern has a significant effect on compressive strength and modulus of elasticity since the reductions for running bonds between same specimen heights are comparable to that of the stack bond doublets vs 5-course prisms. According to the data, to the bond pattern governs the compressive strength across the tested various height to thickness ratio specimens.

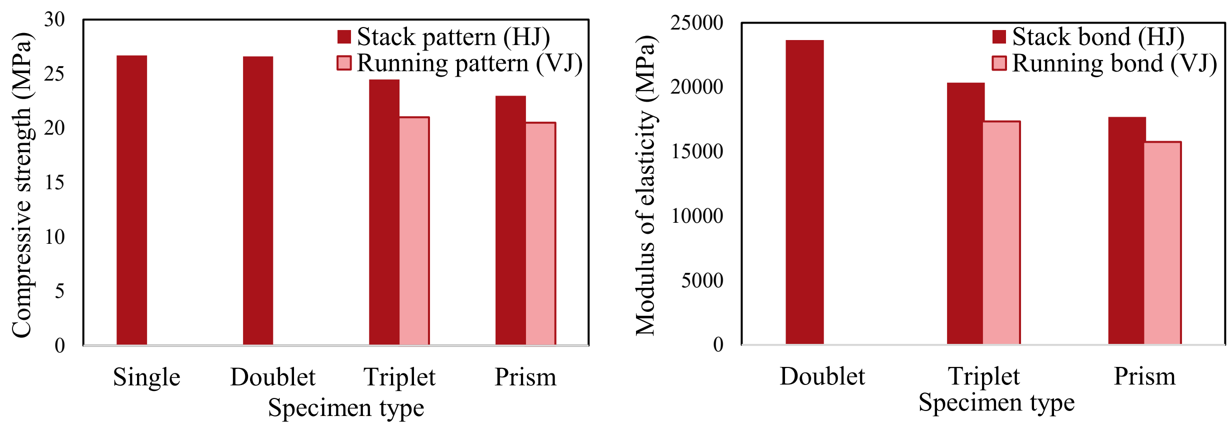

Figure 3.1. Compressive strength and modulus of elasticity across various specimen heights and bond patterns

These trends can be witnessed and further exemplified in Figure 3.2. It is noted that with more mortared joints present in the specimens, the peak force is reached at a higher displacement and a much lower force than for single or doublet assemblies. Also, as seen in Figure 3.3, the modulus of elasticity curves is steeper in slope for most of the stack pattern, a slight decrease in slope for the running bond prisms. This can be related to the failure mechanisms of the concrete masonry assemblies.

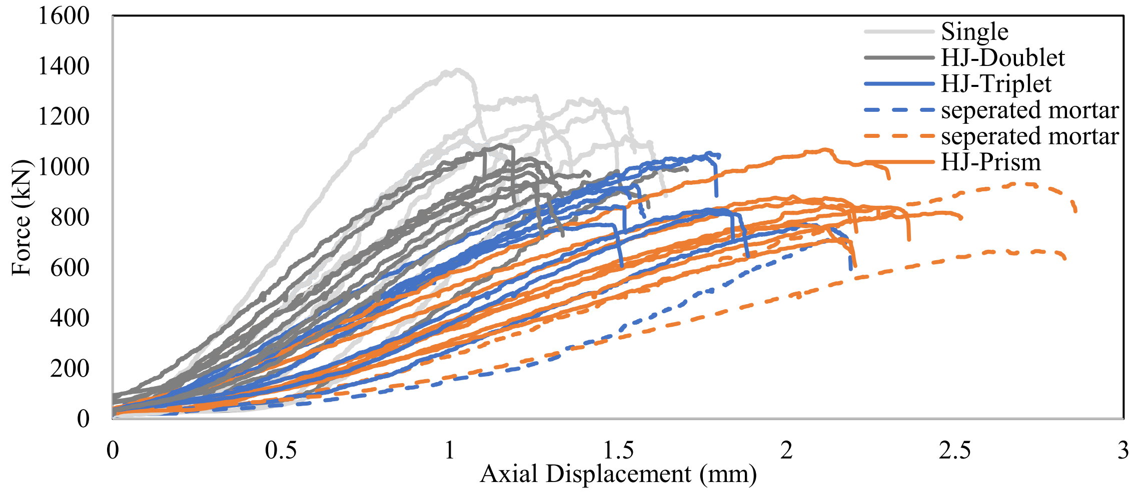

Figure 3.2. Force vs displacement graph of all the stack pattern tested specimens

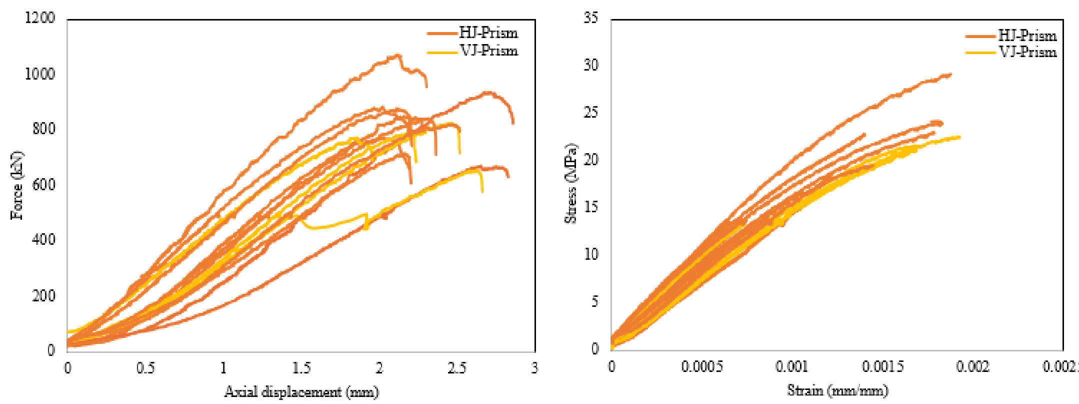

Figure 3.3. Force vs displacement graph and stress vs strain graph of HJ and VJ prisms

As seen in the following figures, there was minimal damage done on all faces of the tested single blocks, while more apparent damage on taller specimens. As the height to thickness ratio increases, the severity of the block failures is evident. The stack bonds (HJ) are more prone to horizontal cracking and spalling in one of the blocks as presented in Figure 3.4. However, Figure 3.5 for the running bond (VJ) shows more diagonal cracking along its longitudinal face. These cracks propagate through more than one block and usually pass through the vertical mortar joints. This failure in the VJ assemblies can be attributed to the weak vertical mortar joint, which may not be capable of resisting the compression as does the horizontal mortar joints due to the direction of loading onto the bond. The higher number of mortar joints present in the assemblies causes more deformation under compression until the cracking becomes significant enough that the peak load is achieved and the test ends.

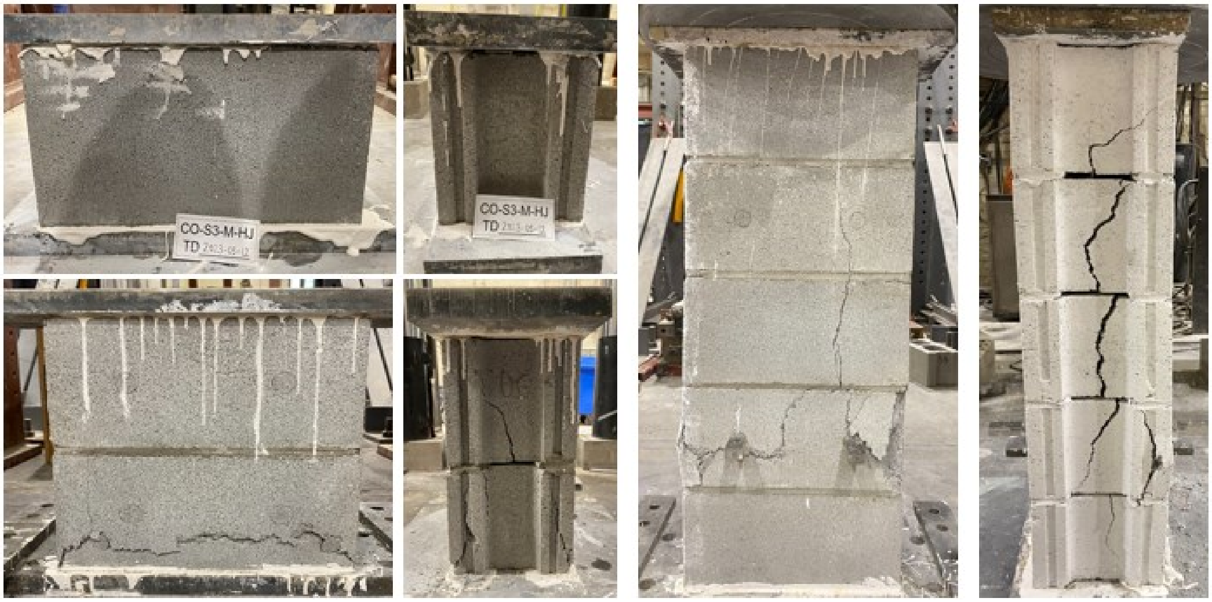

Figure 3.4. Sample compressive failures associated with stack bond pattern

Figure 3.5. Sample compressive failures associated with running bond pattern

These failure mechanisms typical across the specimens are known to vary in severity and crack lengths which can be explained by differential movement between blocks, mortar joints, surface irregularities and imperfection in alignment of blocks which create the potential for load distribution issues across assemblies. A consistent failure across all the specimens is the cracking on the width of the blocks (shortest side). This can be attributed to the Poisson effect which is the expansion of an object in the perpendicular direction to the applied compression. For the compression testing of concrete block assemblies, the concrete tends to expand sideways and creates tensile stresses which makes it prone to cracking as the concrete splits apart horizontally. The failures can sometimes involve a sudden loud cracking noise, while other failures can also occur more gradual with no abrupt noise.

The correction factors as presented in Table D.1 of CSA S304-14 (Figure 1.15) are the conservative factors across the varying height to thickness ratios. Upon performing the compression testing of the masonry assemblies in this experimental research, correction factors were deduced based on the experimental compressive strength data found using the 5-course prism as the benchmark for converting the correction factors. The height to thickness ratios for the tested specimens are 2.05 for doublets, 3.11 for triplets and 5.21 for 5-course prisms, however these ratios are not exact values that account for the mortar joints across the specimens. Since the height to thickness ratio can be interpolated in between the given values in the table from CSA, the correction factors associated with the tested specimens should be 0.853 for doublets, 0.906 for triplets and 1.01 for 5-stack prism. The data and graphs presented above consist of the non corrected data and the comparison between the ideal correction factors from CSA and those found in this research are found in Figure 3.6. The experimental correction factors from this research testing are found by dividing the average peak load of 5-course prisms by the average peak load of the other tested specimens. The experimental factors for the stack patterns are 0.86 for doublets, 0.94 for triplets and 1.0 for HJ-prism, while the VJ-triplet is 0.98 and 1.0 for HJ-prism. The stack pattern results slightly differ from the CSA correction factors; however, the running bond factors differ significantly. These results demonstrate the clear difference between testing of varying height-to-thickness ratio specimens and the importance of bond patterns when considering this thesis' experimental correction factors as compared with the CSA data.

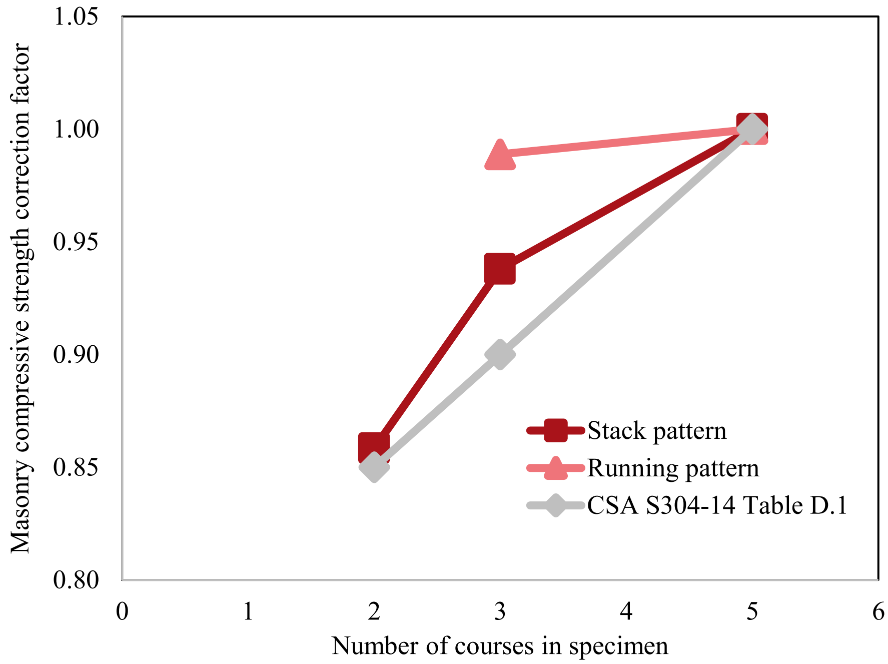

Figure 3.6. Correction factor comparison between experimental compressive strengths and conservative CSA values

3.2 Ties results

The results of all the tested ties will be shown in this section as well as some sample graphs and the types of failure to better demonstrate the observed results. The tabulated values for both BLOK-LOK and FERO in tension and in compression are presented without the necessary factors multiplied to them to show the original data. The factored ultimate strength of ties depicted in the bar graphs in this section includes the 0.9 factor for failure of the tie and the (1-1.64(COV)) factor. The stiffness represented in this section does not have the same factors applied to it since the factors were for strength and there is no reporting in standards. The stiffness values and graphs presented at the end of the results section are the original unaltered data and are presented for both tie types. Also, the average mechanical free play values are recorded for every test and placed in the tabulated results for each tested specimen. The LVDT sensors attached to the tie setup and the displacements measured by the SINTECH machine proved to have corresponding displacements throughout most of the testing.

3.2.1 BLOK-LOK tension

Table 3.2. BLOK-LOK tension data

Tension BLOK-LOK ties	Average displacement in mm at peak force or at 4 mm (COV)	Average force kN between peak force or force at 4 mm (COV %)	Average initial stiffness kN/mm (COV %)	Average mechanical free play (mm)
3”-M-HDG (5)	4.00	1.96 (12.44)	4.47 (16.85)	0.26
3”-L-HDG (5)	4.00	4.01 (6.37)	5.1 (15.51)	0.31
3”-R-HDG (5)	4.00	4.16 (2.45)	6.30 (23.55)	0.29
5”-M-HDG (5)	2.75 (26.73)	1.86 (11.27)	3.91 (6.73)	0.22
5”-L-HDG (5)	4.00	3.95 (2.24)	5.14 (23.94)	0.22
5”-R-HDG (5)	4.00	4.04 (2.62)	6.06 (14.81)	0.19
6”-M-SS (5)	1.20 (25)	2.40 (14.62)	4.77 (6.80)	0.31
6”-L-SS (5)	4.00	5.06 (2.10)	6.27 (8.82)	0.24
6”-R-SS (5)	4.00	5.09 (3.63)	6.47 (5.65)	0.25
8”-M-HDG (5)	2.69 (28.28)	1.88 (2.80)	4.59 (15.25)	0.28
8”-L-HDG (5)	4.00	4.17 (1.32)	5.80 (18.96)	0.22
8”-R-HDG (5)	4.00	4.16 (0.89)	6.45 (14.03)	0.18

Across all tested positions in tension for BLOK-LOK ties and using the test data in Table 3.2, the stainless-steel (SS) tie produced the highest factored ultimate strength in tension as seen in Figure 3.7. The stainless-steel ties were found to be clearly stronger in tension than the other ties across the three positions of tension loading, however there wasn’t that much variation of strength across the different lengths of the ties for the respective positions of load. The position of loading does have an influence on the strength of the tie with the right position having the most noticeable strength for the 3” HDG, 5” HDG and 6” SS ties, while being slightly less for the 8” HDG ties. This strength gain can be due to the left loaded position of the slot being located on the side of the tie with the least amount of steel which is explained by the indentation for the embedment of the corrugated part at the bottom of the tie. This part has fewer available properties of steel and therefore a lower strength resistance. Additionally, the right side was more aligned with the clamping of the bottom of the tie using screws which may provide a slight increase from that location as well. The middle position was always the lowest of the tested positions by 45% for all HDG ties and 43% for SS ties when compared to the strongest tie size. The first peak displacement was mostly after the 4 mm displacement limit from CSA, hence the displacement being 4.00 mm in Table 3.2. The few that had the peak force at less 4 mm had a high COV of around 25%. The middle-loaded positions had 75% of their peak forces reached under 4 mm displacement.

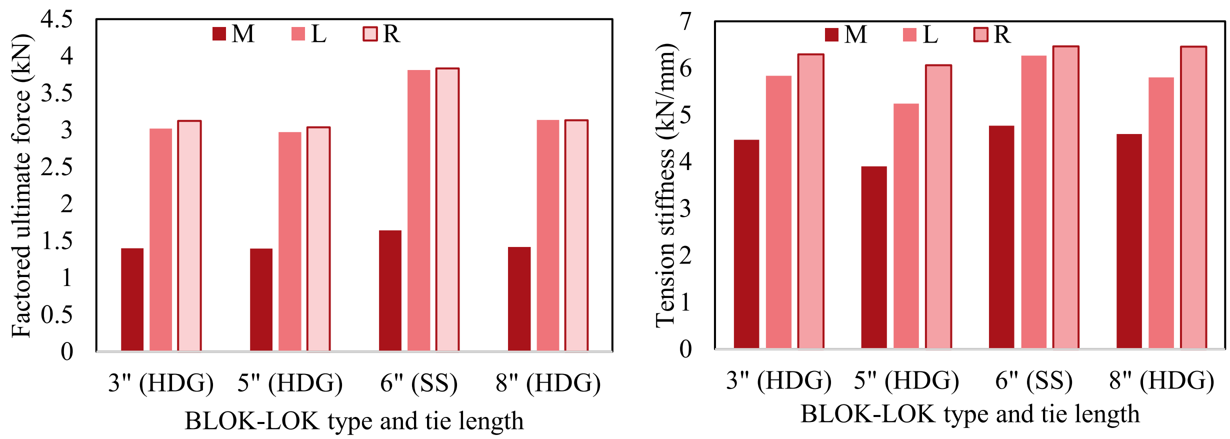

Figure 3.7. BLOK-LOK tension factored strength and stiffness graphs across varying lengths and type of ties

The stiffness of the middle-loaded positions yielded the smallest values across the other positions which is representative since that position is more likely to change with the twisting effect of the adjustable slot which is better explained using representative sample ties found in Figure 3.8. This effect not only reduces the ties' ability for deformation, but it also decreases the factored strength in all the middle-loaded positions. Also, just as with the highest factored strength, all the right-loaded positions have an increased stiffness. The stiffness for the right-loaded position is about 1.43 times greater than the left position for all tie lengths.

As represented by the two sample ties in Figure 3.8, the stainless-steel tie can withstand more deformation and achieve higher loads due to the flexibility of the tie and the ease of shape change witnessed during testing. After achieving the first peak, both curves seem to lose strength, however, the ties quickly carry more load again with the stainless-steel carrying much greater load, almost 2.7 times as much as the HDG tie at a larger displacement.

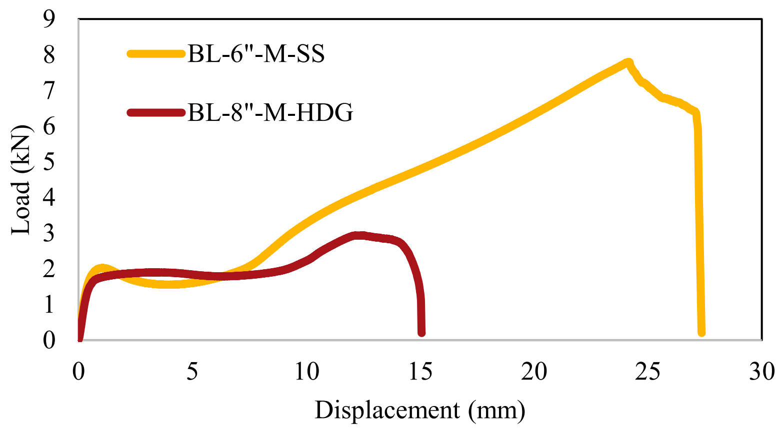

Figure 3.8. Load vs displacement graph for representative ties from 6"-M-SS and 8"-M-HDG

As the ties are pulled in tension, the adjustable slot reaches a point where it starts twisting until it completely turns over onto the FLEX-O-LOK clip, allowing for greater area to be pulled and therefore more strength carrying capacity. The start of the twisting of the tie is characteristic with the initial drop in strength when reaching the peak load and the final drop in strength is attributed to cracks occurring at the corners of the adjustable slot until eventual failure with the tie breaking on either side of the slot. These tension failures are akin to the FERO tie tests across both HDG and SS and some sample stainless steel BLOK-LOK tie tests. Figure 3.9 shows the before and after testing with the evident twisting of the once centered and vertical adjustable slot. The end of the testing of the ties in tension occurred when one of the sides of the adjustable slot broke off from the rest of the tie.

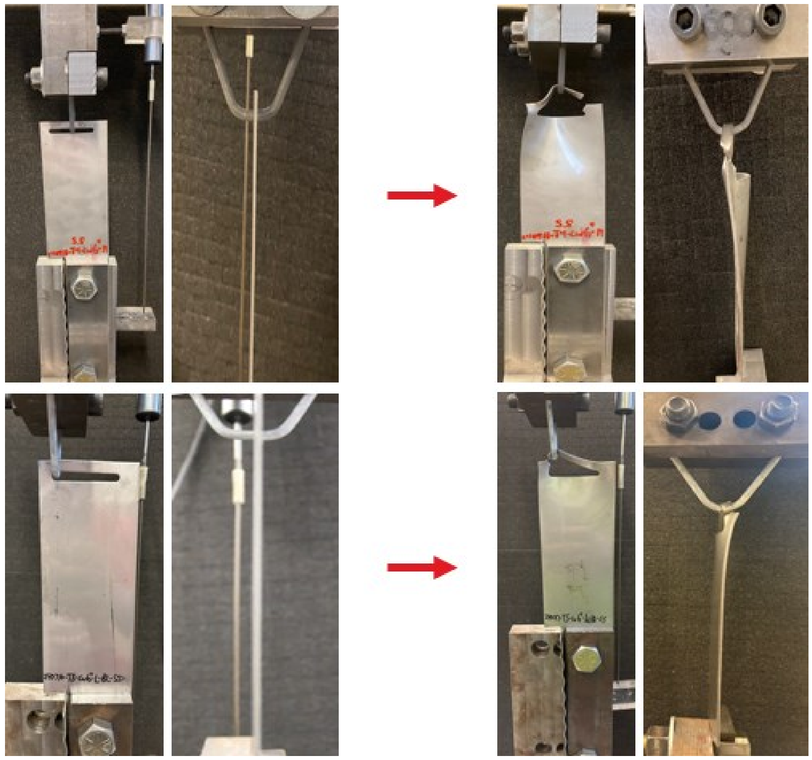

Figure 3.9. Sample twisting failure associated with 6"-M-SS and 6"-L-SS

The twisting of the adjustable slot occurs mainly for the middle position and all the 6” SS loading positions. The other HDG sizes and locations of loading failed with the tie breaking without any twisting, but rather a shearing failure as can be seen with a sample fracture in Figure 3.10. There is no drastic increase in strength since the force continually decreases until reaching failure after its peak load, rather than the adjustable slot tie twisting on its axis along the FLEX-O-LOK clip.

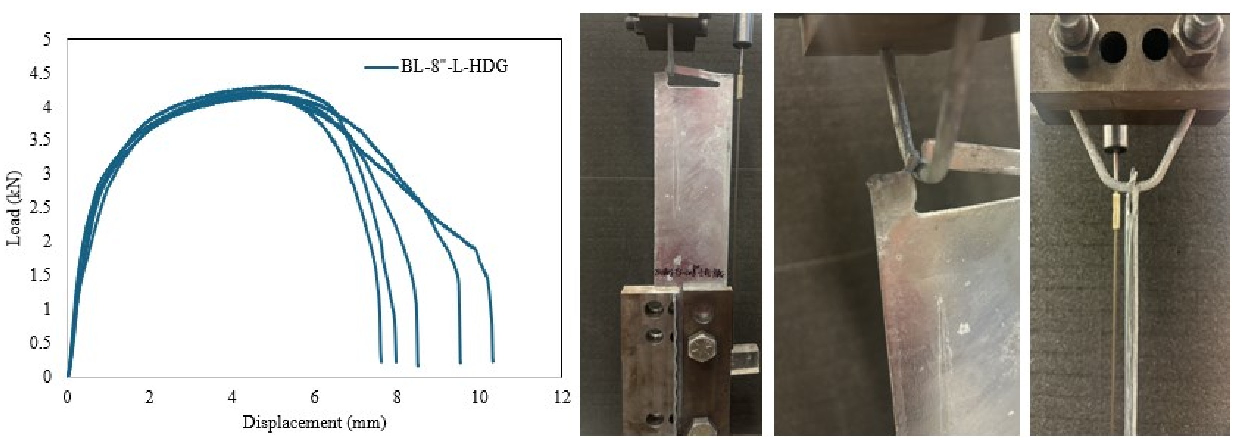

Figure 3.10. Sample failure of the 8"-L-HDG ties

3.2.2 BLOK-LOK compression

In compression, all the ties experienced some level of deflection and buckling as the primary failure factor within the tie and FLEX-O-LOK clip. The ties in compression behave like steel columns in which upon reaching the Euler critical buckling load at its peak load, the load drops as the tie continuously bends until the end of the machine program. The compression loading is halted as the tie bends because the FLEX-O-LOK, which compresses the tie, also meets the upper part of the opening for adjustable slot. As a result, during the later stages of testing, the tie experiences both compression and tension forces. Another reason for stopping the compression test is that the bent tie will eventually touch the steel block setup with the embedded FLEX-O-LOK and will certainly affect the load carrying capacity of the tie.

The larger ties experience more buckling that is considered a permanent deformation, while the smallest tie of 3” experiences elastic deflection within tie with the main permanent deformation happening in the FLEX-O-LOK clip. This deformation in the small tie can be compared to a short column in which it can support more load before reaching critical peak force limit. Therefore, the 3” tie was stronger than the FLEX-O-LOK embedment clip and the other tie sizes in compression across all three loading positions as seen in Figure 3.11. This shows the effects of loading before and after the load was applied to the ties through the FLEX-O-LOK clips. The two images in the middle of figure 3.11show the effects of the deformation of the clip in the shorter tie as compared to the buckling of the longer ties after reaching peak loads. It was also evident that the longer ties deflected favourably on the side of the slot that was loaded, that is, as the clip would compress the tie on the left side, the left of the tie would deflect and buckle with a larger displacement compared to the right portion of the tie.

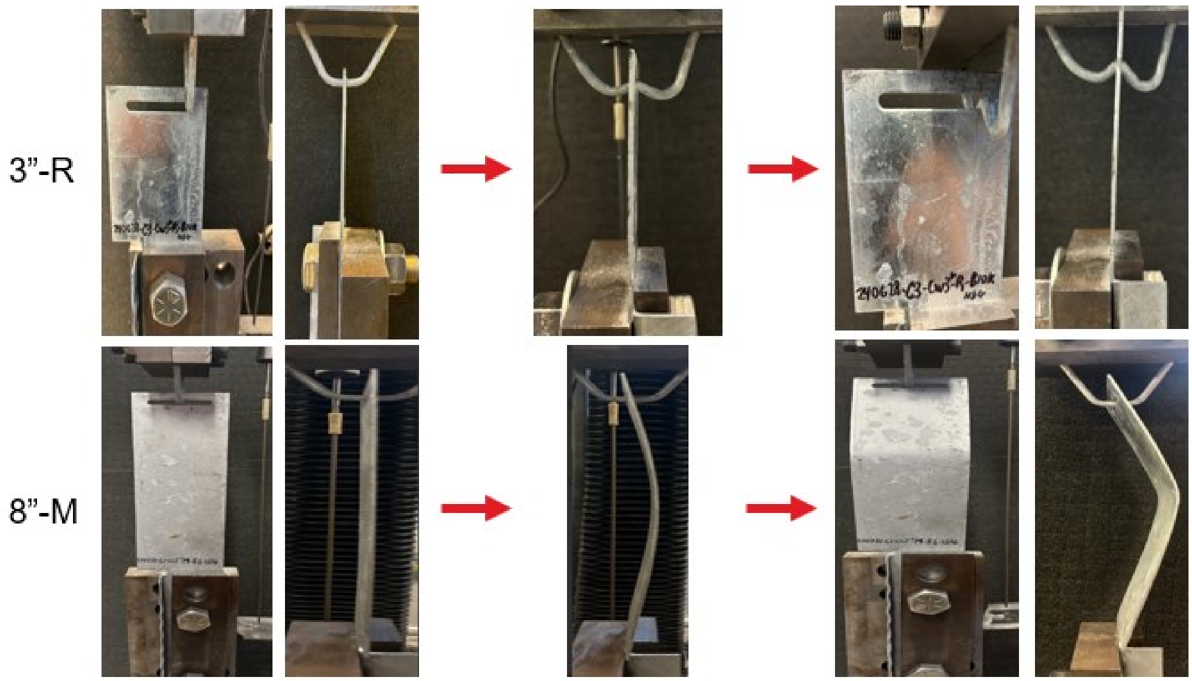

Figure 3.11. Sample compression failures for the 3"-R-HDG and 8"-M-HDG

According to the results in Table 3.3 and Figure 3.12, there is a clear trend with the size of the ties, that is, the ultimate load decreases with the increase in tie length for all three loading positions. The length of tie in compression loading seems to have a better trend than that found in tension for which the size of ties didn’t have a large deviation in factored strength. Considering the different adjustable clip locations along the slot, the middle position had the highest ultimate strength for all the tested ties with the 3”-M being the greatest. The difference between the ultimate strengths of the three clip positions were the closest for the 8”-HDG ties. The ultimate factored force of the 3”-M was 2.7 times greater than the 8”-M. The 6”-M-SS tie was slightly higher than the 5”-M-HDG when theoretically it should be less since the tie is longer, therefore the stainless steel may also influence the strength under compression, however limited tests were performed on SS BLOK-LOK ties to validate the strength. Comparably to the tension tests, the position on the right side of the slot was stronger than the left side potentially due to the asymmetry of the BLOK-LOK ties and setup design. The left position is located on the side of the tie with the least amount of steel due to indentation for the embedment of the corrugated part at the bottom of the tie. Additionally, the right side was more aligned with the clamping of the bottom of the tie using screws which may provide a slight increase from that location as well.

Table 3.3. BLOK-LOK compression data

Compression BLOK-LOK ties	Average displacement in mm at peak force or at 4 mm (COV %)	Average force kN between peak force or force at 4 mm (COV %)	Average initial stiffness kN/mm (COV %)	Average mechanical free play (mm)
3”-M-HDG (5)	3.55 (14.82)	5.30 (1.00)	5.03 (6.10)	0.30
3”-L-HDG (5)	2.78 (9.83)	3.83 (3.86)	6.25 (12.94)	0.22
3”-R-HDG (5)	2.22 (11.63)	3.97 (0.29)	6.62 (22.78)	0.25
5”-M-HDG (5)	1.72 (15.70)	3.29 (9.50)	5.9 (24.01)	0.32
5”-L-HDG (5)	1.703 (22.52)	3.04 (10.08)	6.32 (10.41)	0.30
5”-R-HDG (5)	1.32 (4.00)	3.27 (6.00)	7.62 (9.70)	0.20
6”-M-SS (5)	1.25 (32.10)	3.38 (4.40)	6.25 (18.81)	0.22
6”-L-SS (5)	1.17 (50.20)	2.65 (6.34)	6.29 (9.68)	0.27
6”-R-SS (5)	0.79 (16.83)	3.02 (2.93)	7.73 (12.39)	0.20
8”-M-HDG (5)	1.11 (38.82)	1.96 (3.59)	6.4 (10.35)	0.22
8”-L-HDG (5)	1.38 (40.07)	1.81 (2.30)	5.48 (15.95)	0.21
8”-R-HDG (5)	1.20 (27.50)	1.91 (4.54)	7.71 (12.37)	0.17

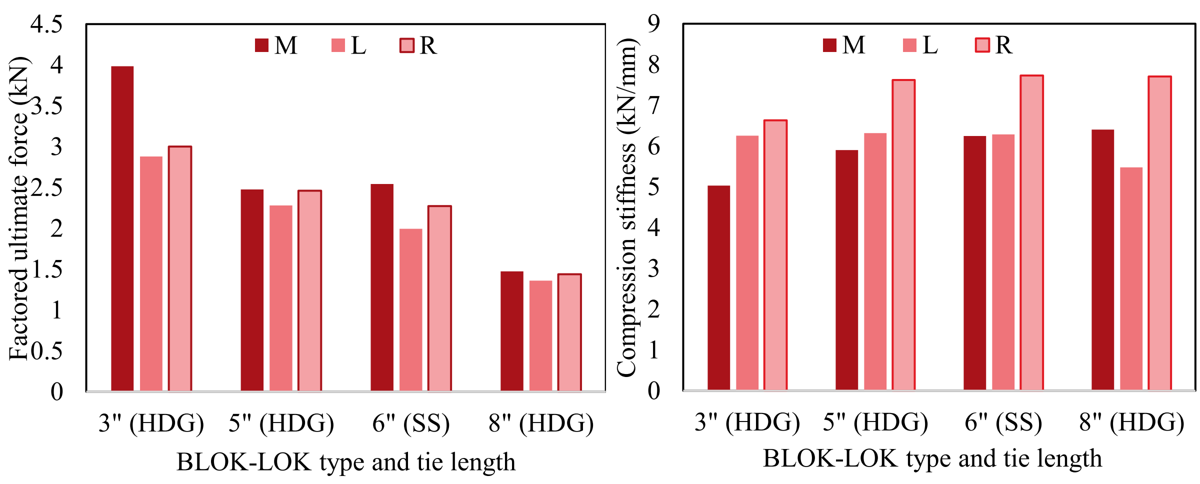

Figure 3.12. BLOK-LOK compression factored strength and stiffness graphs across varying lengths and type of ties

A continued trend for the stiffness in compression is the higher values at the right side of the adjustable slot (Figure 3.12). The stiffness of the middle-loaded and the right-loaded positions seem to continuously increases with length which is consistent with the BLOK-LOK ties in tension. Despite some slight increases in stiffness, the values are all relatively close to each other with no significant change. The stiffness of the ties in compression is greater than the recorded results in tension. Some variation between the stiffness values is more present than the factored ultimate strengths of ties due to the higher COV found with the stiffness data.

The displacement at the peak force occurs before 4 mm for all the BLOK-LOK compression testing (Table 3.3). As the specimen length increases the peak displacements generally decrease since they reach the critical buckling load at fractional loads as compared to the smaller ties which reached the critical buckling load at larger loads. Also, with the 6”-SS and 8”-HDG ties, the COV for displacements was much higher than the smaller ties representing a larger range of buckling points due to length and material properties. The Figure 3.13 shows the significant difference between peak forces and corresponding displacement for the largest tie length of 8” and the shortest of 3”. The 3” tie reaches a higher peak load at a much later displacement than the 8” tie which buckled at smaller peak load and earlier in displacement due to its governing buckling failure in the longer steel tie.

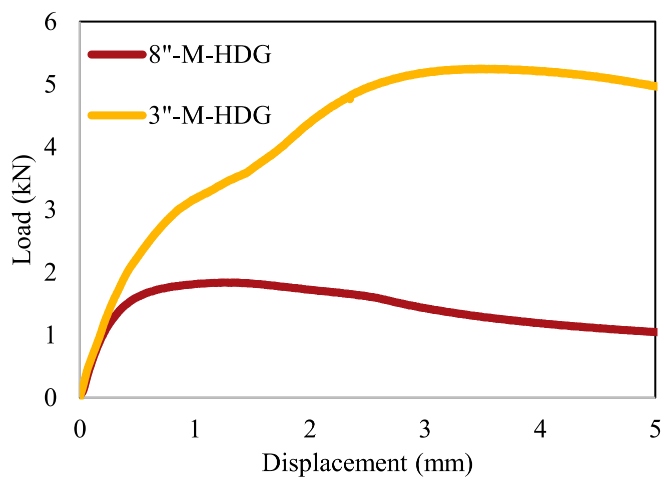

Figure 3.13. Comparison of compression load vs displacement of the longest and shortest length of tie

3.2.3 FERO tension

With the FERO factored strength tension tie tests, the tests are similar to the BLOK-LOK ties in which there isn’t a large deviation in strength across the lengths for the respective loaded positions, however, the FERO ties are much weaker than the BLOK-LOK ties (Figure 3.14). This can be attributed to the percent of steel that makes up the ties. The BLOK-LOK ties are completely made up of steel, while the FERO ties have symmetrically and strategically placed holes to promote a higher R-value and meet insulation needs of structures. These holes may allow for smaller average steel cross-section and carrying capacity of the FERO ties, affecting both the strength and stiffness tension loaded ties. All the ties experienced the twisting effect at the adjustable slot under tension load. The twisting effect was sometimes not as pronounced in the force vs displacement graphs since the initial cracking of the ties occurred before the adjustable slot had the chance to fully twist over onto the V-tie and therefore didn't allow for increased carrying capacity. This was mostly seen with the HDG ties, while the flexibility of the SS ties allowed for more carrying capacity. The stainless-steel advantages for the ties were also noted since 67% of the SS ties are greater than the same lengths in HDG with the 155 mm-M-SS yielding the strongest strength among the ties.

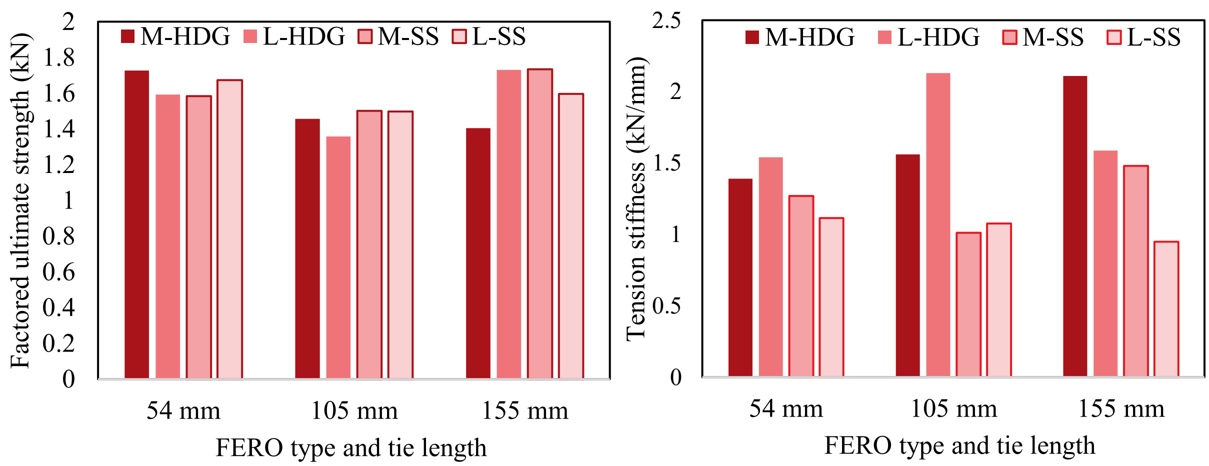

Figure 3.14. FERO tension factored strength and stiffness graphs across varying lengths and type of ties

As for the stiffness of the FERO ties in tension, the SS ties have mostly smaller values than the HDG sizes. This result can be due to the increased flexibility and the observed ability to change shape more easily than the HDG ties during testing. Prior to testing these ties, a sample of HDG and SS ties were bent using a vice and the SS ties were found to be more malleable, hence the results found in the stiffness graph of Figure 3.14. The left-loaded position of the ties was mostly found to have the highest stiffness as compared to the middle-loaded positions which had the smallest stiffness except for the 155 mm. Similar stiffness trend to the BLOK-LOK results in tension, yet with some slight deviations in stiffness across the lengths due to higher COV and tests such as the 105 mm -L-HDG and 155 mm-M-HDG yielding greater and consistent stiffness results

The average peak displacements occurred after the 4 mm limit, with most of the peaks transpiring at around a 10 mm displacement, therefore the 4 mm displacement and corresponding force was recorded in

Table 3.4. These tension results were like the data of the BLOK-LOK ties tested in tension since the peak loads mostly occur after the 4 mm limit from CSA.

Table 3.4. FERO tension data

Tension FERO ties	Average displacement in mm at peak force or at 4 mm (COV %)	Average force kN between peak force or force at 4 mm (COV %)	Average initial stiffness kN/mm (COV %)	Average mechanical free play (mm)
54mm-M-HDG (5)	4.00	2.30 (5.71)	1.39 (4.10)	0.48
54mm-L-HDG (5)	4.00	2.12 (9.13)	1.54 (19.75)	0.21
54mm-M-SS (5)	4.00	2.21 (12.47)	1.27 (5.20)	0.67
54mm-L-SS (5)	4.00	2.29 (11.56)	1.11 (28.62)	0.19
105mm-M-HDG (5)	4.00	1.94 (4.59)	1.56 (14.49)	0.25
105mm-L-HDG (5)	4.00	2.01 (15.18)	2.13 (19.09)	0.25
105mm-M-SS (5)	4.00	2.02 (10.66)	1.01 (17.80)	0.44
105mm-L-SS (5)	4.00	1.99 (3.46)	1.08 (12.25)	0.31
155mm-M-HDG (5)	4.00	1.87 (4.93)	2.11 (19.12)	0.23
155mm-L-HDG (5)	4.00	2.30 (3.31)	1.59 (14.06)	0.28
155mm-M-SS (5)	4.00	2.30 (3.57)	1.48 (14.69)	0.42
155mm-L-SS (5)	4.00	2.12 (6.30)	0.95 (10.73)	0.21

The Figure 3.15 shows the before and after of the twisting of the adjustable slot and the initial fracture which leads to failure with the two images in the middle demonstrating the governing failures. As the adjustable slot tie starts to twist along the V-tie clip, cracks propagated from the slot until eventual full fracture of the tie when the tie completely twists on its axis.

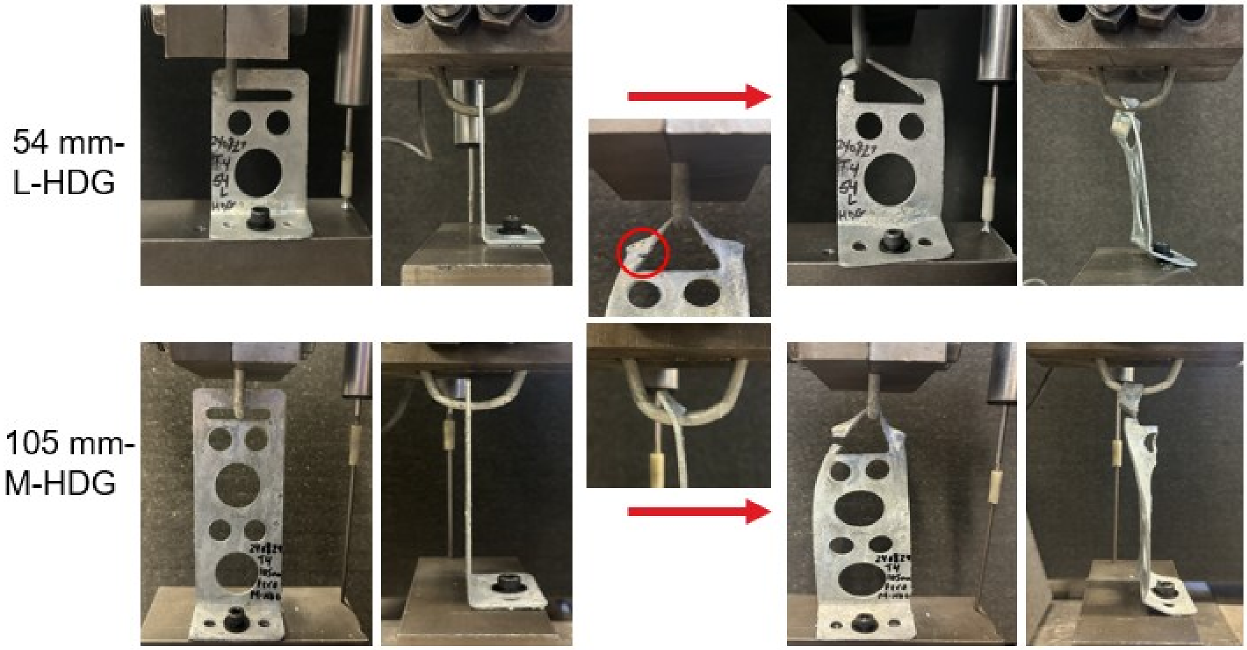

Figure 3.15. Sample FERO tension failure mechanisms for the 54 mm-L-HDG and 105 mm-M-HDG

3.2.4 FERO compression

The compression tests of FERO ties demonstrated the same decreasing factored strength with increasing tie size typical of the BLOK-LOK compression testing (Figure 3.16). Also, the middle-loading of the HDG ties had the greatest factored strength with the difference between the strength of the 54 mm M-HDG and the 155 mm M-HDG being 2.57 kN which translates to a 3.85 times strength reduction for the longest HDG tie size. The holes in the FERO ties influence the factored strength since the strength gain for the BLOK-LOK 3”-M-HDG was only 2.7 times more than the 8”-M-HDG. This shows that the FERO ties are weaker in compression for similar proportion in sizes of the ties tested from both companies. The stainless-steel ties do not have a distinguishable advantage over using the HDG ties and have less force resistance for every position and length when compared to HDG.

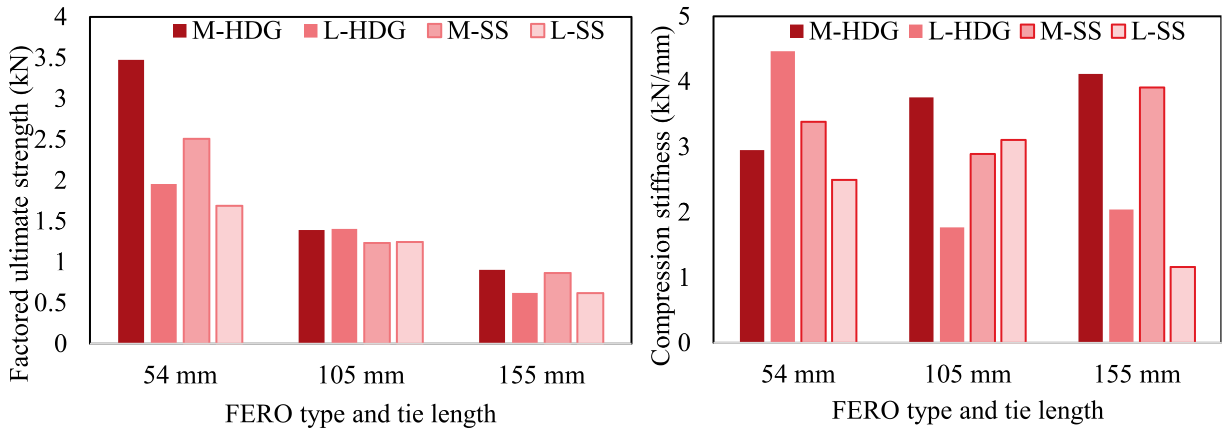

Figure 3.16. FERO compression factored strength and stiffness graphs across varying lengths and type of ties

The stiffness values for the compression of the FERO ties is much less than the BLOK-LOK as discovered with the tension ties as well. The difference between HDG and SS ties is evident, as two out of three tie lengths in both middle and left positions show lower stiffness in the SS ties. The largest stiffness was found in the 54 mm-L-HDG with 4.47 kN/mm, while the smallest was the 155 mm-L-SS with 1.16 kN/mm. The stiffness values still seem to follow a similar trend as the other tests however a higher stiffness COV was seen across the FERO compression data which allowed for more deviation between results and defined fewer clear patterns among the ties.

Following the pattern of the BLOK-LOK compression tests, the displacements at the peak load generally decrease with increasing tie lengths across both steel types of HDG and SS (Table 3.5). Most of the SS ties reached their peaks at lower displacements than the HDG ties for both the middle and left loaded positions. This can be due to the SS being more visually malleable under compression loading than the HDG ties.

Table 3.5. FERO compression data

Compression FERO ties	Average displacement in mm at peak force or at 4 mm (COV %)	Average force kN between peak force or force at 4 mm (COV %)	Average initial stiffness kN/mm (COV %)	Average mechanical free play (mm)
54mm-M-HDG (5)	3.03 (6.66)	4.62 (3.60)	2.95 (11.87)	0.28
54mm-L-HDG (5)	1.15 (19.89)	2.60 (2.11)	4.47 (19.32)	0.23
54mm-M-SS (5)	2.96 (36.71)	3.36 (10.36)	3.39 (18.57)	0.9
54mm-L-SS (5)	1.38 (4.16)	2.24 (1.69)	2.50 (18.60)	0.24

105mm-M-HDG (5)	1.06 (21.40)	1.85 (2.07)	3.76 (3.00)	0.25
105mm-L-HDG (5)	1.08 (19.34)	1.89 (10.66)	1.77 (30.01)	0.27
105mm-M-SS (5)	1.02 (10.39)	1.64 (3.93)	2.89 (7.93)	0.26
105mm-L-SS (5)	0.73 (17.46)	1.66 (9.70)	3.10 (18.03)	0.25
155mm-M-HDG (5)	1.15 (24.70)	1.29 (13.44)	3.24 (15.15)	0.32
155mm-L-HDG (5)	1.15 (31.65)	1.05 (20.92)	2.05 (28.10)	0.25
155mm-M-SS (5)	0.5 (1.43)	1.15 (1.78)	3.91 (3.26)	0.38
155mm-L-SS (5)	1.33 (7.18)	0.82 (6.67)	1.16 (7.27)	0.19

The failure mechanisms with compression testing are consistent with BLOK-LOK, that is the buckling of the ties across all positions and lengths. All the ties buckled with permanent deformation, meaning none of the tested ties returned to the original shape after releasing the machine's applied load like the behaviour of the elastic deformation for the 3" BLOK-LOK. As seen with the BLOK-LOK, the side with the applied loading is apparent as the tie bends and deflects more on the left loading applied side of the adjustable slot. These sample buckling effects can be identified in Figure 3.17.

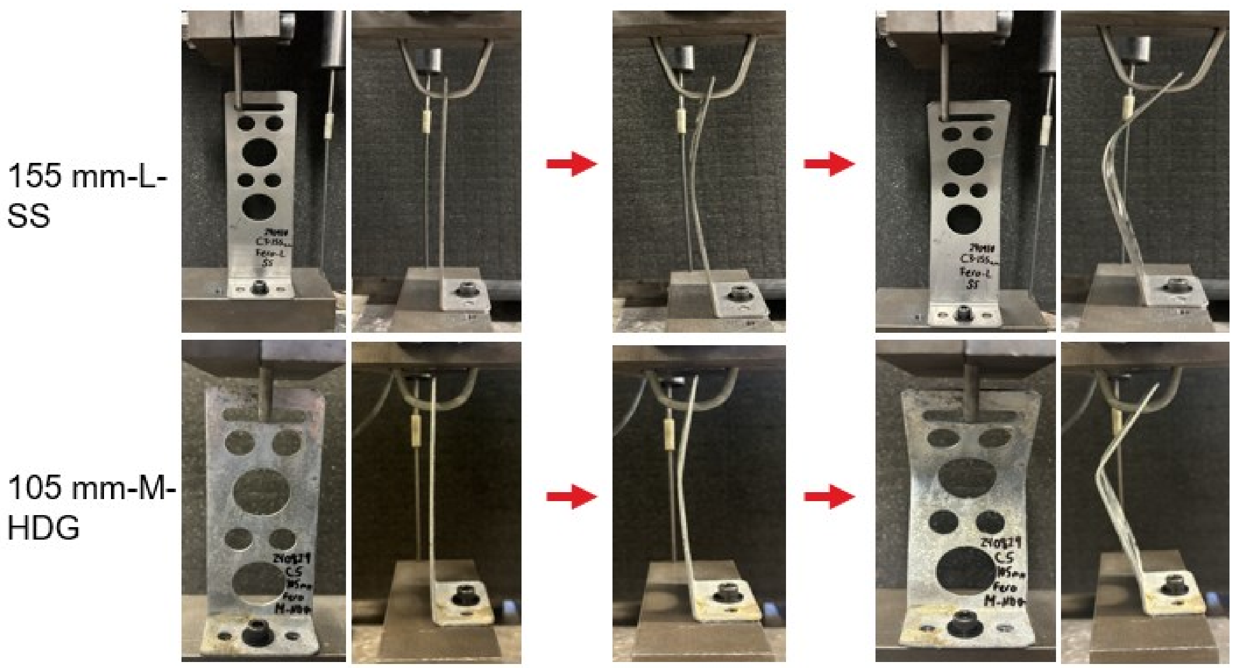

Figure 3.17. Sample FERO compression failure mechanisms for the 155 mm-L-SS and 105 mm-M-HDG

All the compression of the middle loaded 54 mm stainless steel ties underwent a slipping effect of the V-tie clip in the adjustable slot shortly after reaching the peak load. This slippage of the clip can be witnessed in Figure 3.18 with the drop in force after reaching the peak load due to the shifting along the slot which can be seen in the image. The load increased after the load quickly dropped. This is attributed to the imbalance of forces created as the clip was in contact with both the top and bottom of the slot. The compression load pushed the clip onto the tie and compressed it while the top part of the adjustable slot opening was being pushed in the upwards direction by the V-tie clip.

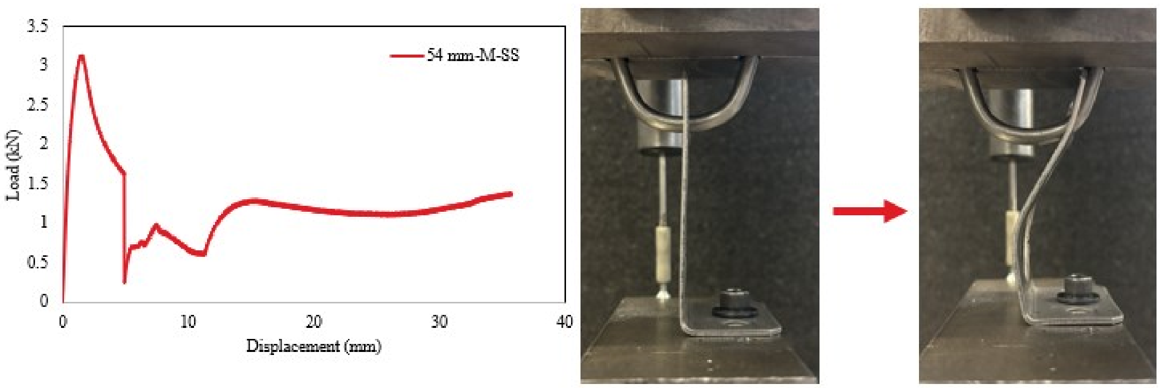

Figure 3.18. Stainless steel adjustable slot slips along the V-tie clip under compression testing of 54 mm ties

4 Conclusions

This experimental research aims at assessing the mechanical characteristics of concrete masonry block assemblies under compression loading as well as the tension and compression of a large range of modern adjustable ties. The research campaign tested 53 concrete masonry block assemblies and 240 modern adjustable metal ties from the companies BLOK-LOK and FERO.

The following points can be made based on the compression testing of the concrete block results performed throughout the research:

- The stack bond pattern has a strength reduction of 9.5% and 6.5% for the increase in assembly height from doublets to triplets and triplets to 5-course prisms, respectively.
- The transition from triplets to 5-course prism for running bonds has a 2% decrease in compressive strength.
- For the comparison between the same height of stack and running bonds, a sizeable increase in strength for the stack specimens of 15% and 10% for the triplets and the 5-course prisms, respectively.
- For the modulus of elasticity of stack patterns, a decrease of 34% from doublet to 5-course prism and 15% from triplet to 5-course prism.
- The modulus comparison between the same height of stack and running bonds is 17% increase for stack triplets and 12.4% for five-course prisms.
- A 10% reduction in modulus of elasticity for the running bond between the triplets and 5-course prism.
- The experimental results comparison to the correction factors demonstrates relatively close values for the stack pattern while the triplet factors for the experimental running bond differ significantly.

The CSA mandates the testing of running bond assemblies and the correction factors are conservative values from running bond testing, however, as the results show, the correction factors may need adjustment to create optimized testing for structural standards and design. These conclusions allow for better understanding of the combined effects of height-to-thickness ratios and the bond patterns with the potential for further masonry assembly testing to update the correction factors for future structural development and research. The implementation of modern compressive strength results and updates to standards can help optimize and prevent over or under conservative load design of structures which can lead to more cost-effective and performance based sustainable construction practices. A note concerning the completed experimental research is the fewer tests performed on the running bonds which may influence the collected data.

The following points are the highlights of the cavity wall testing results:

- The larger ties maintain similar tensile strength as smaller ties, yet they show significant strength reduction in compression across both BLOK-LOK and FERO.
- FERO stainless-steel ties have more factored strength than the HDG ties in tension, with 67% showing higher strength, and the 155 mm M-SS tie being the strongest.
- The largest FERO middle HDG tie shows a 3.85x strength reduction compared to the smallest HDG, while the smallest BLOK-LOK middle HDG is only 2.7x stronger than the 8”-M-HDG under compression.
- The BLOK-LOK 6"-M-SS tie had slightly higher compression strength than the 5"-M-HDG, suggesting stainless steel may influence strength despite longer length, however few tests of SS are not able to validate strength.
- The right-side slot positions of BLOK-LOK were stronger than the left side, likely due to tie asymmetry, more steel and better alignment with fixed support (screws) located along the right side.
- Under the tension loading, all the FERO ties underwent twisting effect at the adjustable slot, while the BLOK-LOK was mainly the middle position and SS ties.
- Most of the middle-loading of the BLOK-LOK and FERO HDG ties has the greatest factored strength under compression loads.
- BLOK-LOK ties show 3x tensile increase in stiffness and 2.05x increase in compression compared to the inferior FERO ties.
- The FERO ties have strategically placed holes to enhance R-value and insulation, however, this design also reduces the steel cross-section and lowers the strength and stiffness under loading.

The adjustable slot twisting under tension suggests potential future design improvements to the ties. A design change can consist of increasing the steel thickness near the slot for the tie to carry a higher initial tensile and compressive strength to avoid twisting and initiating failure. The additional thickness surrounding the adjustable slot could increase the carrying capacity behaviour of the rest of tie subjected to the force being applied by the clip. This may allow for ties to carry a higher initial tensile and compressive force due to it being able to distribute these loads over a larger cross-section slot area when loaded with the FLEX-O-LOK or V-tie clips. The larger ties seem to allow for similar tensile strength as the smaller ties, however for compression testing, the lower peak load due to buckling for the longer ties is apparent with more deformation as compared to smaller ties. The stiffness compression results across the FERO ties have more variation along the results and it may be attributable to the greater COV of the specimen tests associated with the FERO compared to the BLOK-LOK tie results. The holes in the FERO ties promote an increased R-value but may also allow for more deviation in the behaviour and results for the stiffness data. Through this experimental testing, understanding the individual strengths and stiffness of a large range of ties under loads at various adjustable positions creates a catalogue of data that can be put in practice depending on needs of structures. As energy needs and building performances continually evolve, so does the need for increasing cavity wall widths to allow for more insulation. This research can be an accessory to future testing of adjustable ties in concrete doublets and both small and large cavity walls with varying cavity widths to understand the combined effects of strength and stiffness on complete material assemblies. The knowledge of the resistances of the tie load alignment within the mortar joints of brick veneers and loadbearing backup wall will undoubtedly provide an optimization to the cavity wall and ties design to accommodate wider and more sustainable cavities.

5 References

Al-Sanea, S. A., et al. (2003). "Heat transfer characteristics and optimum insulation thickness for cavity walls." Journal of Thermal Envelope and Building Science 26(3): 285-307.

Canadian Standards Association. (2014). “CSA A165 (R2018) CSA Standards on concrete masonry units.” CSA Group.

Canadian Standards Association. (2014). “CSA-A179-14 (R2019) Mortar and grout for unit masonry.” CSA Group.

Canadian Standards Association. (2014). “CSA A370:14 (R2023) Connectors for masonry.” CSA Group.

Canadian Standards Association. (2014). “S304-14 (R2019) Design of masonry structures.” CSA Group.

DiDomizio, D., et al. (2024). "From mass masonry to veneer: The evolution of cavity wall design." Construction Specifications Institute (CSI).

Dizhur, D., et al. (2015). "Historical development and observed earthquake performance of unreinforced clay brick masonry cavity walls." SESOC Journal 28(1): 55-67.

Drysdale, R. G. and A. A. Hamid (1979). "Behavior of concrete block masonry under axial compression." Journal Proceedings.

Fortes, E. S., et al. (2015). "Relationship between the compressive strength of concrete masonry and the compressive strength of concrete masonry units." Journal of Materials in Civil Engineering 27(9): 04014238.

Giaretton, M., et al. (2016). "Construction Details and Observed Earthquake Performance of Unreinforced Clay Brick Masonry Cavity-walls." Structures. 6 (2016) 159–169.

Hamid, A. A. and A. O. Chukwunenye (1986). "Compression behavior of concrete masonry prisms." Journal of Structural Engineering 112(3): 605-613.

Hatzinikolas, M., et al. (1982). "Strength and behaviour of metal ties in 2-wythe masonry walls." Alberta Masonry Institute.

Hatzinikolas, M., et al. (1983). "Ties in large cavity and veneer masonry walls." Alberta Masonry Institute.

Hatzinikolas, M. and J. Warwaruk (1991). "Connecting cavity walls." Brick and Block Masonry 2: 996-1003.

Ismaiel, M., et al. (2022). "Thermal resistance of masonry walls: a literature review on influence factors, evaluation, and improvement." Journal of Building Physics 45(4): 528-567.

Mahajan, B. (2021). "Cavity Wall: Understanding Thickness, Uses, and Construction Methods." Civiconcepts. https://civiconcepts.com/blog/cavity-wall. Accessed 28 September 2024.

Martins, A., et al. (2017). "Brick masonry veneer walls: An overview." Journal of Building Engineering 9: 29-41.

Mohamad, G., et al. (2011). "Study of the compressive strength of concrete block prisms: stack and running bond." Revista IBRACON de Estruturas e Materiais 4: 347-358.

Pasquantonio, R. D., et al. (2020). "Experimental and numerical characterization of the interface between concrete masonry block and mortar." Revista IBRACON de Estruturas e Materiais 13(03): 578-592.

Potts, P. (2022). "Designing masonry cavity walls." CONSTRUCTION CANADA. https://www.constructioncanada.net/designing-masonry-cavity-walls/. Accessed 19 September 2024.

Rizaee, S., et al. (2016). "Comparison of compressive strength of concrete block masonry prisms and solid concrete prisms." 16th International Brick and Block Masonry Conference, IBMAC, Padova, Italy.

Sarhat, S. R. and E. G. Sherwood (2014). "The prediction of compressive strength of ungrouted hollow concrete block masonry." Construction and Building Materials 58: 111-121.

Schendelpest (2020). "Why do I have mice in my walls in Norman, OK?" Schendel. https://www.schendelpest.com/blog. Accessed 17 September 2024.

Sigva, A. (2018). "Does cavity wall insulation actually work?" Cavitech UK LIMITED. https://cavitech-uk.com/blog/does-cavity-wall-insulation-actually-work/. Accessed 20 September 2024.

Skroumpelou, G., et al. (2018). "Mechanical characterization of wall tie connection in cavity walls." Proceeding of the 10th Australasian masonry conference, Sydney, Australia.

Sparling, A., et al. (2021). "Climate Change Adaptation of CSA Standards for Masonry Connectors." Canadian Society of Civil Engineering Annual Conference, Springer.

THE CONSTRUCTOR. (2020). "Rat Trap Bond – Construction, Advantages, and Disadvantages."Theconstructor.org.https://theconstructor.org/building/rat-trap-bond-construction-advantages-disadvantages/37334/. Accessed 21 October 2024.

Williams, C. and A. Hamid (2005). "In-Plane Stiffness and Strength of Adjustable Wall Ties." 10th Canadian Masonry Symposium.